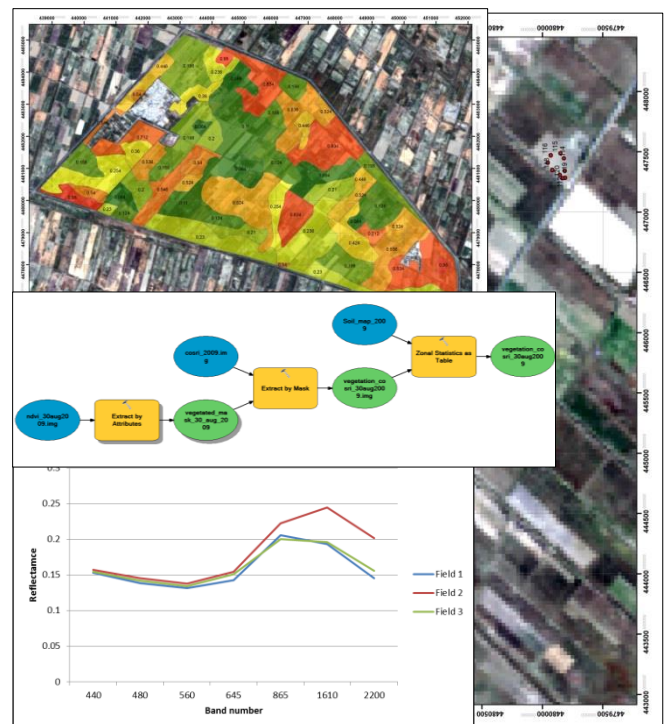Centre for Geo-Information

Thesis Report GIRS-2014-05

Soil salinity assessment using Remote Sensing and GIS techniques in Syrdarya province of Uzbekistan

Konstantin Ivushkin

June 2014

WAGENINGEN UNIVERSITY
WAGENINGEN UR

Soil salinity assessment using Remote Sensing and GIS techniques in Syrdarya province of Uzbekistan

Konstantin Ivushkin

Registration number 89 06 23 383 130

<u>Supervisors</u>:

Dr Alim Pulatov

Dr Harm Bartholomeus

A thesis submitted in partial fulfilment of the degree of Master of Science

at Wageningen University and Research Centre,

The Netherlands.

June 2014

Tashkent, Uzbekistan

Wageningen, The Netherlands

Acknowledgement

Abstract

High salts content in soil remains a big problem for agriculture. Uzbekistan located in semiarid and arid region and this problem particularly acute here. High soil salinity leads to inhibition of crop growth and, as consequence, decrease of yields. The aim of the research was to test existing techniques of soil salinity assessment using GIS and remote sensing tools and find the best for environments of Syrdarya province in Uzbekistan. The research can be divided into two major parts: analysis of bare soil reflectance and reflectance of vegetation. Landsat 5 and 8 images were used for calculations and analysis. For bare soil several indices, found in literature, were tested and spectral signatures of areas with different soil salinity analysed. For vegetation relations of two indices, NDVI and COSRI, were analysed and spectral signatures of vegetation growing on areas with different soil salinity. Two datasets were used in the calculations: data collected especially for this thesis and secondary data from the salinity map of the Research Institute for Soil Science and Agrochemistry. None of the indices from literature showed significant correlation, in both datasets. The highest R value (-0.41) is found between the satellite data of the bare soil with the map of the Research Institute for Soil Science and Agrochemistry. The same situation occurs with the analysis of the spectral signatures – no difference was observed between signatures of slightly, moderately and highly saline soils. With vegetation reflectance we receive more promising results. The highest R value -0.57 is observed for the COSRI index and in the dataset with secondary data. The correlation with NDVI images is a little bit lower (R = -0.53). From the results of this research we conclude that using vegetation indices as a proxy parameter for soil salinity is more promising in environments of Syrdarya province than the use of bare soil indices.

Abbreviations

COSRI – Combined Spectral Response Index

DN – Digital number

EC – Electrical conductivity

FAO – Food and Agriculture Organization of the United Nations

NDVI – Normalized difference vegetation index

NIR – Near infrared spectral band

PCA – Principal Component Analysis

RGB – Red, green, blue colour composition

RS – Remote Sensing

SAVI – Soil-adjusted Vegetation Index

SWIR – Short wave infrared spectral band

TDS – Total dissolved salts

TIR – Thermal infrared spectral band

TOA – Top of the atmosphere reflectance

USGS – United States Geological Survey

WCA – Water Consumer Association

Table of Contents

List of figures

List of tables

1. Introduction

Soil salinity is a serious environmental problem, especially in arid and semi-arid regions. Danger of this problem lies in the fact that high level of salts in soil inhibits growth and development of all common agricultural crops. Salinization is a major form of land degradation in agricultural areas, where information on the extent and magnitude of soil salinity is needed for better planning and implementation of effective soil reclamation programs. Statistics about the extent of world salt affected areas vary according to authors; however, general estimates are close to 1 billion hectares, which represent about 7% of the earth's continental extent (Ghassemi et al. 1995). In addition to these naturally salt affected areas, about 77 million ha have been salinized as a consequence of human activities (secondary salinization), with 58% in irrigated areas. On average, 20% of the world's irrigated lands are affected by salts, but this figure increases to more than 30% in countries such as Egypt, Iran and Argentina (Ghassemi et al. 1995). At global scale, soil salinization is spreading at a rate of up to 2 million ha per year, which offsets a significant portion of the crop production that is otherwise achievable by using the best management practices at a system level (Abbas et al. 2013).

Soil salinity in irrigated areas is becoming a serious problem for agriculture, especially in arid and semi-arid climates. Saline soil conditions have resulted in reduction of the value and productivity of considerable areas of land throughout the world. Salinity commonly occurs in irrigated soil because of the accumulations of soluble salts introduced from the continuous use of irrigation waters containing high or medium quantity of dissolved salts (Al-Hassoun 2010).

For Uzbekistan this problem is very important too. Sixty nine percent of the total irrigated land in Central Asia and 50.5% area in Uzbekistan are already affected by various degrees of soil salinity (Bucknall et al. 2003). There is near 2 million hectares of high salinity areas. Salinization processes most intensively progress in Karakalpakstan Republic, Bukhara province, Sirdarya province and some parts of Fergana valley. The last decades rapid changes in area affected by secondary salinization occurred in Karakalpakistan, Khorezm and Syrdarya regions. The risk of soil salinization is further aggravated due to the rising water table, as a result of high irrigation water application in the fields and the poorly managed drainage channel system (Toderich et al. 2008).

Salinization reduces cotton yields by 20-30% on slightly salinized lands, 40-60% on moderately salinized lands, and 80% or more on heavily salinized lands (UNDP 2009). According to the World Bank estimates, annual losses in agricultural output in Uzbekistan due to land salinity/degradation are estimated to equal USD 31 mln., while the economic losses due to agricultural land taken out of use equals roughly 12 million USD (Bucknall et al. 2003). By more recent assessments salinity, uneconomic pumping lifts, and poor water quality lead to abandonment of 20,000 ha of irrigated land per year. Further, the salinity problem costs Uzbekistan about 1 billion USD per year (The World Bank 2007).

According to statistics for 2003 – 2008 in the Syrdarya province the lands affected by salinization, especially human caused increased from 87 to 95%. Among them more than 80% of the soils are heavy saline. All these lands being partly used as low productive gradually are out from the irrigated agricultural use and abandoned by farmers. In the Mirza chul steppe the area of arable lands has reduced from 805,000 ha in 1991 to 531,000 ha in 2006 (Toderich et al. 2008).

Management of sector policies and programs is the responsibility of the Ministry of Agricultural and Water Resources, which includes major water management and forestry departments. This Ministry has branches in all provinces and districts. However, the Ministry has no unit for environmental issues. The Ministry is advised by a Council on Rational Utilization of Water and Land Resources, Development of Irrigation and Increasing of Soil Fertility, consisting of eminent academicians and practitioners, which meets occasionally. It recently supported organizing irrigation operation and maintenance on a command area basis and expanding water users associations (WUAs) (The World Bank 2007).

One of the important projects in the agricultural area of Uzbekistan is creation of Land Reclamation Fund. The Fund is responsible for financing construction, reconstruction, repair and maintenance of interregional and inter-farm open collectors, vertical drainage, horizontal drainage, pump stations, and monitoring stations. The Ministry of Agriculture and Water Resources (MAWR) is responsible for repair and maintenance of on farm drainage systems. Work of this fund and some other projects helps to decrease severity of the salinity problem. Starting from 2008 area of highly and moderately saline soils are decreased by 113 thousand hectares (Karimov 2014).

1.1 Role of Remote Sensing and GIS

To keep track of changes in salinity and anticipate further degradation, mapping and monitoring is needed so that proper and timely decisions can be made to modify the management practices or undertake reclamation and rehabilitation measures. Mapping and monitoring of salinity means first identifying the areas where salts concentrate and secondly, detecting changes in this occurrence (Robbins and Wiegand 1990). The implementation of sustainable agricultural, hydrological, and environmental management requires an improved understanding of the soil, at increasingly finer scales. Conventional soil sampling and laboratory analyses cannot efficiently provide this information, because they are slow, expensive, and could not retrieve all temporal and spatial variability (Zribi et al. 2011).

Remotely sensed data and Geoinformatics caused a revolution in research related to agriculture, land, water, marine and geomorphology. It helps the researchers to facilitate the investigations, assessments and may lead to more understanding of sustainable development. Remotely sensed data has a great potential for monitoring dynamic processes, including salinization. The ability to predict soil salinity accurately from remote sensing data is important because it saves labour, time, and effort when compared to field collection of soil salinity data (Robbins and Wiegand 1990).

The integration of remote sensing data, in the form of satellite imagery, with the GIS has boosted up the ability of delineating and mapping soil salinity (Al-Mulla 2010). Remote sensing was proved useful in detecting salinity trend using Landsat enhanced thematic mapper plus (ETM +) data along with other field data and topographical maps to show the spectral classes and salt-affected areas. Salinity map created using NDVI and some auxiliary data showed 67% correlation with EC values (Ochieng et al. 2013). Satellite images can be used to get insight in the dynamics of the salinity and water

logging in the area. But good knowledge of cropping pattern, meteorological conditions at recording time of the image and agricultural practices are needed in order to correctly assess the results (Singh and Somvanshi 2012).

In general, techniques for remote sensing salinity assessment can be divided into two groups. A first group is so called direct estimation. Here assessment is done using reflectance of soil itself, when it is free of vegetation. The second group is indirect estimation. Here it means that vegetation is used as an indirect indicator of soil salinity. Next two sections are divided according to these two groups of techniques. Hyperspectral data analysis is highlighted in separate section, since no experiments were done with hyperspectral images during this research. But this section can be considered important to show possibilities for future development of this research topic.

1.2 Soil salinity assessment using reflectance and thermal emissivity of bare soil

The topic of remote sensing for soil salinity assessment already was raised in Uzbekistan more than 10 years ago. Karavanova et al. (2001) used simple spectral classification on images from Russian satellites for Uzbekistan area. Images were composed of green, red and NIR spectral bands. It allows separating of five classes of soil salinity with accuracy up to 70%. But this is most recent work that is available, no more recent research can be found for Uzbekistan.

1.2.1 Salinity indices

Very convenient technique for remote sensing salinity assessment is calculation of different salinity indices. And several works had been done in this direction. One of the earliest indices found in literature is salinity index proposed by Tripathi et al. (1997). It is calculated as band 3/band 4, bands of Landsat 5 (7) is meant. In work of Indo-Dutch Network Project (2002) was proposed three salinity indices: SI1 = band 5/band 7, SI2 = (band 4-band 5)/(band 4+band 5) and SI3 = (band 5-band 7)/(band 5+band 7). These indices became point of interest in some future articles. Al-Khaier (2003) presented salinity index, calculated for Aster satellite images. It has an accurate detection for overall salinity (R = 0.86) on the bare agricultural areas. But since 2008 these bands of Aster sensor does not operable anymore. Nevertheless almost the same bands available on Landsat sensors and for Landsat 5 or 7 this index will look like (band 5 − band 7)/(band 5 + band 7), which makes this work still useful. But in this formulation it is repeating of index SI3 from Indo-Dutch Network Project (2002). Douaoui et al. (2006) test more than 10 indices (including different vegetation and salinity indices) for its correlation with EC values for study area in Algeria. Highest correlation coefficients were achieved for two salinity indices: $SI1 = \sqrt{G * R}$ with R =

0.50 and $SI3 = \sqrt{G^2 + R^2}$, with R = 0.49. Bouaziz et al. (2011) also tested several indices and best correlation with salinity levels was found in index named SI2, calculated as $SI2 = \sqrt{G^2 + R^2 + NIR^2}$. Also in this research authors showed usability of linear spectral unmixing to increase accuracy of assessments and correlation coefficients. Abbas et al. (2013) proposed 4 indices for new Indian satellite IRS-1B LISS-II. They calculated as *B/R*; *(B–R)/(B+R)*; *(G*R)/B*; and the last one $\sqrt{B * R}$. All this indices also can be recalculated using Landsat images, since it uses only three main bands: blue, green and red. Correlation coefficients for these indices vary from 0.64 to 0.82.

Table 1. Summary of indices found during literature research ("band" are bands of Landsat 8 and R, G, B, NIR – spectral bands)

Index formula	Author	Correlation coefficient (R)
band 4/band 5	Tripathi et al. (1997)	N/A
band 6/band 7	Indo-Dutch Network Project (2002)	N/A
(band 5-band 6)/(band 5+band 6)		N/A
(band 6-band 7)/(band 6+band 7)		N/A
$\sqrt{G * R}$	Douaoui et al. (2006)	0.50
$\sqrt{G^2 + R^2}$		0.49
$\sqrt{G^2 + R^2 + NIR^2}$	Bouaziz et al. (2011)	0.58
B/R	Abbas et al. (2013)	In a range from 0.64 to 0.82
(B–R)/(B+R)		
(G*R)/B		
$\sqrt{B * R}$		

1.2.2 Importance of different wavelengths and spectral bands for salinity assessment

But even more researches were devoted to revealing sensitivity of different parts of the spectra to soil salinity and classification techniques based on this sensitivity data.

Zehtabian et al. (2002) reveal during their research that infrared Landsat 7 bands (band 5 and band 7) are very efficient in determining the salt crust and salt blisters from different classes of soil. Howari (2003) discover that there are 5 regions of the mean spectra that exhibited distinct absorption features and high variability in the salts content in soil. They were located around 1000, 1400, 1900, 2200, and 2300 nm, and can be used for salt type identification and presence of salts in general. Eldiery et al. (2005) used ordinary least squares model on Ikonos data to assess soil salinity. The results show that, the green band, the near infrared band, and the near infrared band divided by the red band ratio are strongly related to soil salinity. R^2 value achieved was 0.52. Shrestha (2006) showed in his research that mid-infrared (band 7) and near-infrared (band 4) bands of Landsat 7 images have high association with observed EC. Bannari et al. (2007) tested EO-1 ALI data potential for soil salinity discrimination. The results showed that the SWIR region (bands of 1550-1750 nm 2080-2350 nm) is a good indicator, being more sensitive to different degrees of slight and moderate soil salinity and sodicity. The importance of the thermal band of Landsat images was reflected in work of Alavi Panah et al. (2008). Based on the results obtained from this study, the TM thermal band is important for improving the classification accuracy of gravely saline soil and crusted soil surface. Mehrjardi et al. (2008) proposed regression model for band 3 of Landsat 7 images. This model formulated as $y = 0.001e^{0.058x}$. It was used in Yazd-Ardakan Plain in Iran and showed correlation coefficient R=0.58.

Also usability of different image processing techniques for salinity assessment was tested. Pattanaaik et al. (2008) applied principal component analysis on Landsat images to delineate severe saline areas. The RGB colour composite was generated, in which PC1 of NIR is displayed in red and PC1 of Red and PC1 of Green is displayed in green and blue respectively. In this composition dark tones showed clearly the severe salt-affected areas. Wu et al. (2008) showed land cover supervised classification technique, including areas affected by salinity in different degrees. Results showed that the spectral response of salt-affected soils, especially strongly and moderately saline soils, is higher than the other classes in all bands of Landsat images. Overall accuracy was 90.2%.

In work of Gutierrez and Johnson (2010) Landsat 5 (7) band 5 (1550-1750 nm) was used and proved to be one of the two best bands as an indicator for salts; band 7 (2080-2350 nm) being the other. They choose simple threshold for band 5 for classification, and pixels with reflectance values in range 0.46-0.51 was classified as salt affected.

Iqbal et al. (2010) stated that maximum reflectance of salt affected soils was observed in 10500 -12500 nm range and minimum reflectance in the 760 - 900 nm range. And ratio of TIR and NIR is useful for salt prone land detection. Abbas et al. (2013) mention that spectral response of the salt-affected soils higher than those of normal soils. Salty soils reflected more incident light energy in visible spectrum and this response extremely useful in the segregation of saline soils. Noroozi et al. (2012) stated that mid-infrared band and visible blue band are strongly associated with the observed salinity levels. Koshal (2012) in his work studied soil reflectance in green, red and near infrared bands. It was observed that salt affected soils have high spectral values in red and near infrared bands. This observation is extremely useful as it helped in distinguishing of salt affected soil, waterlogged soil and normal

soils. Severe salt affected soils had the highest reflectance in all three bands (green, red and infrared) followed by moderate salt affected soil. Normal soils have a low reflectance in the red band. That helped to distinguish the image characteristics of normal soils from salt affected lands.

As can be seen from above mostly all currently available bands in multispectral sensors have some importance in salinity detection. But also noticeable that NIR band mentioned very often.

Despite the great variety, most of the indices and regression models show good correlation only on specific soils and under certain conditions. For example two indices (NDSI and index proposed by Al-Khaier (2003)) was tested by author during the internship, and no good correlation was found for soils in Uzbekistan. This makes relevant research work related to finding good index or model for Uzbekistan soils. And also no work was found on this topic based on Landsat 8 images. In Landsat 8 bands widths were changed, also new bands were added. This gives new possibilities for index calculations and regression models that should be tested in Uzbekistan.

Use of hyperspectral sensors can give better results. Mainly because such type of sensors are able to detect noticeable absorption features of salts. Hyperspectral sensors are a powerful and versatile tool for monitoring environmental stress because of the continuous sampling and the high spectral resolution (<5 nm) (Zhang et al. 2011).

Mashimbye et al. (2012) used hyperspectral images and showed in their research partial least square regression models for salinity assessment with R^2 values up to 0.85. Also interesting thing in this research that untransformed individual band at 2 257 nm can be used for salinity prediction with R^2 value 0.60.

Weng et al. (2010) find out that the increases in absorption intensity at 1 144, 1 416–1 447, and 1 911–1 945 nm became more pronounced as the salinity level increased. This phenomenon was reversed at around 1 800, 2 203, and 2 345 nm, as spectral absorptions increased with the decrease of salinity level. The correlation coefficients were negative in the spectral ranges from 1 447 to 1 608 nm and from 1 941 to 2 092 nm but changed to positive from 1 780 to 1 850 nm and 2 153 to 2 254 nm. Therefore, these bands were sensitive to soil salinity. They chose these two spectral regions for the construction of soil salinity spectral indices because the contrast was the largest in those regions. According to these calculations best index $SSI = (B_{2203} - B_{2052})/(B_{2203} + B_{2052})$ was developed. Lower case numbers – wavelengths of reflectance used, in nm. This index was developed based on laboratory spectral measurements, then applied for Hyperion EO-1 data. Achieved R^2 value was 0.627.

But acquiring of hyperspectral images very costly and most of them not available for free public access, small amount of available images can't cover whole Earth surface. This makes them not feasible in many cases. And because this technology, especially if used from air and space domains, has encountered some problems (e.g., the availability of sensors, retrieval of non-laboratory quality data, skilled personnel to process the data, and the relatively high cost) only limited studies have used this means for soil applications (Ben-Dor et al. 2009). But from this section also can be seen that NIR and SWIR spectral regions mentioned more often than others.

1.3 Soil salinity assessment using reflectance of vegetation

As it was already mentioned, soil salinity has negative effects on plant growth and decrease yields. In the vascular plants water-based soil solutions surrounding their roots become part of the plant's delicately-balanced aqueous environment. The stresses imposed by salinity relate to ion composition and to ion concentration within the plants. When dissolved salt concentrations in soil solutions increase, water energy gradients decrease, making it more difficult for water and nutrients to move through root membranes and into the plant. The rate of water and solute uptake slows, but does not cease. With time, the solute-rich soil water increases ionic concentrations within the plant's aqueous transportation stream. This osmotic effect, encountered at the root membrane, applies at all the plant's internal membranes served by its conductive tissue. Internal excesses of particular ions may cause membrane damage, interfere with solute balances, or cause shifts in nutrient concentrations. Some specific symptoms of plant damage may be recognized especially in the leaves: colour change, tip-burn, marginal necrosis, succulence, etc. (Volkmar et al. 1998).

And all these changes can be detected by remote sensing also. In general, decrease of reflectance in NIR band can be corresponded with health of vegetation and, as a collateral indicator, with salinity levels.

If involving vegetation into calculation, one index for salinity was found in literature. Fernández-Buces et al. (2006) proposed COSRI index and test it using Landsat 7 data. This combined index calculated as COSRI = [(band 1 + band 2)/(band 3 + band 4)]*NDVI. When exponential model used this index shows $R^2 = 0.83$, when plotted against EC values.

In Uzbekistan research about using remote sensing of vegetation for salinity assessment was implemented by Akramova (2008). She used NDVI and

SAVI as indicators of soil salinity for agricultural fields in Uzbekistan. Results showed R^2 values for NDVI 0.67 and for SAVI 0.63 when EM-38 values were averaged per field.

Also simple classification was used on agricultural fields for salinity detection. Elhaddad and Garcia (2009) used unsupervised classification for corn fields. This helped to classify Landsat images into 9 classes, with salinity levels in range 0-10 dS/m. A relatively strong correlation between vegetation cover and soil salt content, an R^2 greater than 0.74, was found according to regression analysis in work of Wang et al. (2013). Some researchers propose to combine different vegetation indices, NDVI in most cases, and salinity indices. Processing of this data in GIS environments can increase accuracy of salinity maps (Dehni and Lounis 2012). Other researchers propose to combine vegetation indices and water indices to create land cover maps, which also include salinity levels. Ding et al. (2011) propose to combine NDVI, MNDWI (modified normalized difference water index) and some PCA manipulations to create decision tree that can classify three salinity classes: Non-saline soil, Middle and light saline soil, Severe saline soil.

Several researches were done with hyperspectral images. Hamzeh et al. (2013) formulated three indices for salinity assessment using vegetation as a proxy. Indices were calculated for Hyperion sensor images and formulas are: $SWSI1 = \frac{R803-R681}{\sqrt{R905+R972}}$; $SWSI2 = \frac{R803-R681}{\sqrt{R1326+R11507}}$; $SWSI3 = \frac{R803-R681}{\sqrt{R972+R1174}}$. R^2 values achieved were up to 0.68.

Zhang et al. (2011) proposed several VIs sensitive to salt stress in plants, but all of them is species sensitive. R^2 values ranged from 0.5 to 0.58 for different plant species.

Dutkiewicz et al. (2009) used hyperspectral images of HyMap, Hyperion and CASI sensors to map soil salinity. They used several absorption features of

salt minerals and vegetation, which allows using these methods on barren lands and vegetated areas. Several hyperspectral vegetation indices was developed by Zhang et al. (2011) especially for salinity detection. These indices showed good performance calculated for different species, including halophyte species.

 But, as any indirect indicator, use of vegetation data for soil salinity assessments introduces additional inaccuracies. For example decrease of NDVI and any other suppression of vegetation can be caused by many factors, like water availability, wrong use of fertilizers, etc. And all this brings a problem to find exact values of different vegetation indices for specific soils and vegetation species, which can be related with actual salinity levels.

1.4 Problem definition, research questions and hypothesis

Despite the great variety, most of the indices and regression models show good correlation only on specific soils and under certain conditions. For example two indices (NDSI and index proposed by Al-Khaier (2003)) was tested by author during the internship (Ivushkin 2012), and no good correlation was found for soils in Syrdarya province of Uzbekistan. This makes relevant research work for finding good index or model for Uzbekistan soils. And also no work was found on this topic based on Landsat 8 images. In Landsat 8 bands widths were changed, also new bands were added. This gives new possibilities for index calculations and regression models that should be tested in Uzbekistan.

Also no clear method for vegetation reflectance analysis in relation to soil salinity was found. As any indirect indicator, use of vegetation data for soil salinity assessments introduces additional inaccuracies and it is important to see how we can use this data in a right way (Akramova 2008).

One more important point is how to use existing data (maps, reports, etc.) of research organisation in Uzbekistan to combine them with RS and GIS techniques and to show possibilities of these tools in application to soil salinity studies. There are salinity maps for most agricultural areas in Uzbekistan and it is important to see how we can use them as a ground truth data for this research.

To answer these problems next research questions were formulated:

1. Which of the existing remote sensing based models/indices gives the best results for soil salinity assessments on test sites in Syrdarya region based on bare soil reflectance?

2. Which of the existing remote sensing based models/indices gives the best results for soil salinity assessments on test sites in Syrdarya region based on vegetation reflectance?

3. To what extent standard salinity map values, used in Uzbekistan, correlate with different remote sensing derived salinity indices values?

And next hypothesis was formulated:

Analysis of spectral reflectance of bare soil and vegetation in Syrdarya province can help in assessment of salinity level on study area.

2. Materials and methods

2.1 Study area

This research was implemented on the test site in Syrdarya province of Uzbekistan on Bobur WCA. This is one of the highly salt affected areas in Uzbekistan. Syrdarya Province is located in the centre of the country on the left bank of the Syrdarya River on a vast piedmont plain, from the south adjacent to the foothills of the Turkestan range. It borders with Kazakhstan, Tajikistan, Toshkent Province and Jizzakh Province. It covers an area of 5,100 km², mostly desert, with Starving Steppe taking up a significant part of the province's area. Flat terrain broke by softly pronounced deflection going from the southeast towards the Kyzyl-Kum sands. Deflection is divided into a number of depressions, of which largest are Agachatinskaya, Dzhetysai - Sardoba and Shuruzyakskaya. Central part of the valley is lined by lake-alluvial proluvial sediments. Eastern part is composed of loess and alluvial deposits. The plain has a slow natural groundwater flow that under irrigation
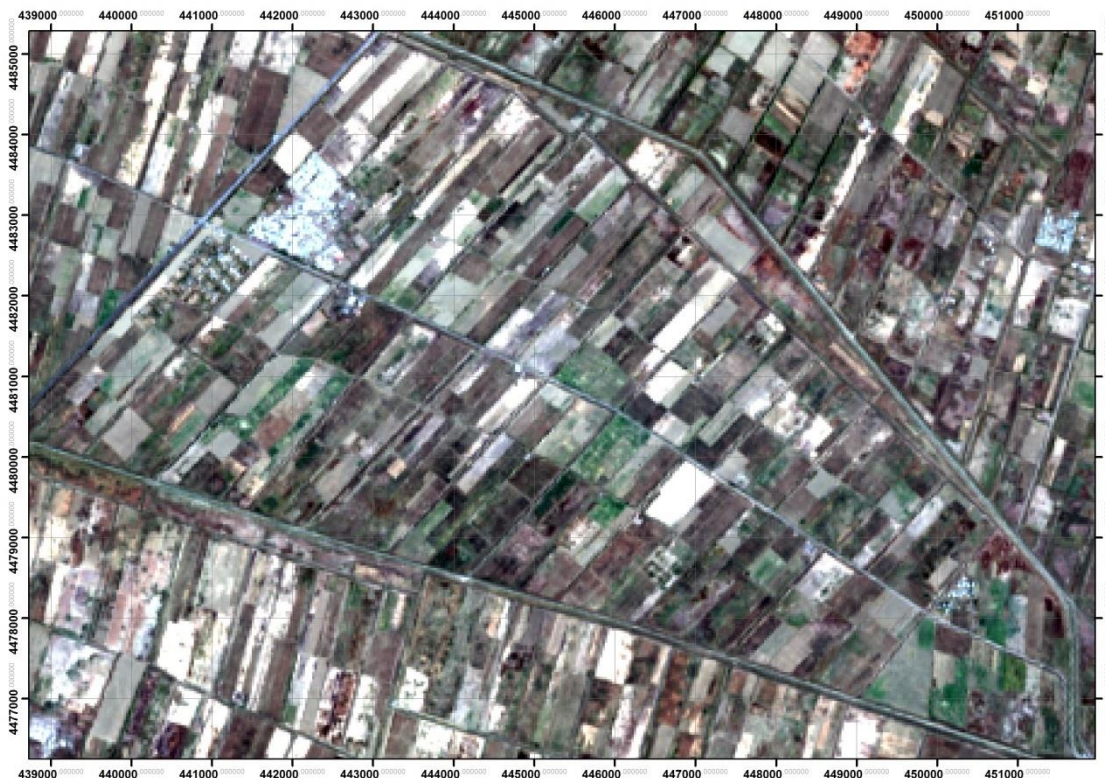
Figure 1. Bobur water consumers association area (Landsat 8 image)

leads to water table uprising and deterioration of vertical water exchange. This lead to transition of automorphic soils into semi-hydromorphic and hydromorphic soils and appearance of secondary salinization. Groundwater level is different in different parts of the plain. On terraces above the floodplain of the Syrdarya river water table depth is 1-2.5 m, in central parts of a plains – 2-3 m, in depressions and hollows level little higher. Especially high level of groundwater is observed in the floodplain of the Syrdarya river (0.5-1 m).

The area is in Turan soil-climatic province, in a zone of light grey soils. Over time due to changes in hydrological conditions most of them transformed into grey-meadow and meadow soils prone to secondary salinization. Currently, light grey soils cover only small part of the province. Predominant part of the irrigated lands accounts for grey-meadow and meadow soils with small plots of swampy meadow soils. Some of them relates to gypsum-bearing soils. Gypsum-bearing soils occur mainly in the southern districts (Goskomgeodezkadastr 2010).

In the province most of the agricultural lands are affected by different degrees of salinity: 9.4% of extremely saline soils, 59.9% of highly saline soils and 20.9 of moderately saline soils (State Research Institute of Soil Science and Agrochemistry 2005).

Population of the province is estimated to be around 648 000. Economy based on cotton and cereal crops, with strong reliance on irrigation and cattle breeding. Minor crops include forage plants, vegetables, melons, gourds, potatoes, maize, variety of fruit and grapes. Industry consists of construction materials production, irrigation equipment industry and raw-cotton processing.

Test fields are located on Bobur WCA, which is the association of several farmers. Bobur WCA area has a mean annual temperature of -5°C in winter and +28°C in summer and an average annual precipitation of 180-220 mm. Agricultural lands are irrigated by channels. Main crops grown in the WCA are cotton (Gossypium hirsutum L.) and winter wheat (Triticum aestivum L.).

2.2 Description of the map used as secondary data source

Together with the soil data collected during thesis work, secondary data was used. As a secondary data a map of the Research Institute of Soil Science and Agrochemistry was used. We received a scanned version of this map in .jpeg format, which was not georeferenced. The map contains 25 zones with TDS values for each zone and a salinity class based on local classification.

The map was georefernced in ERDAS Imagine, and vectorised in ArcGIS (Figure 2). The map was dated by the year 2009.
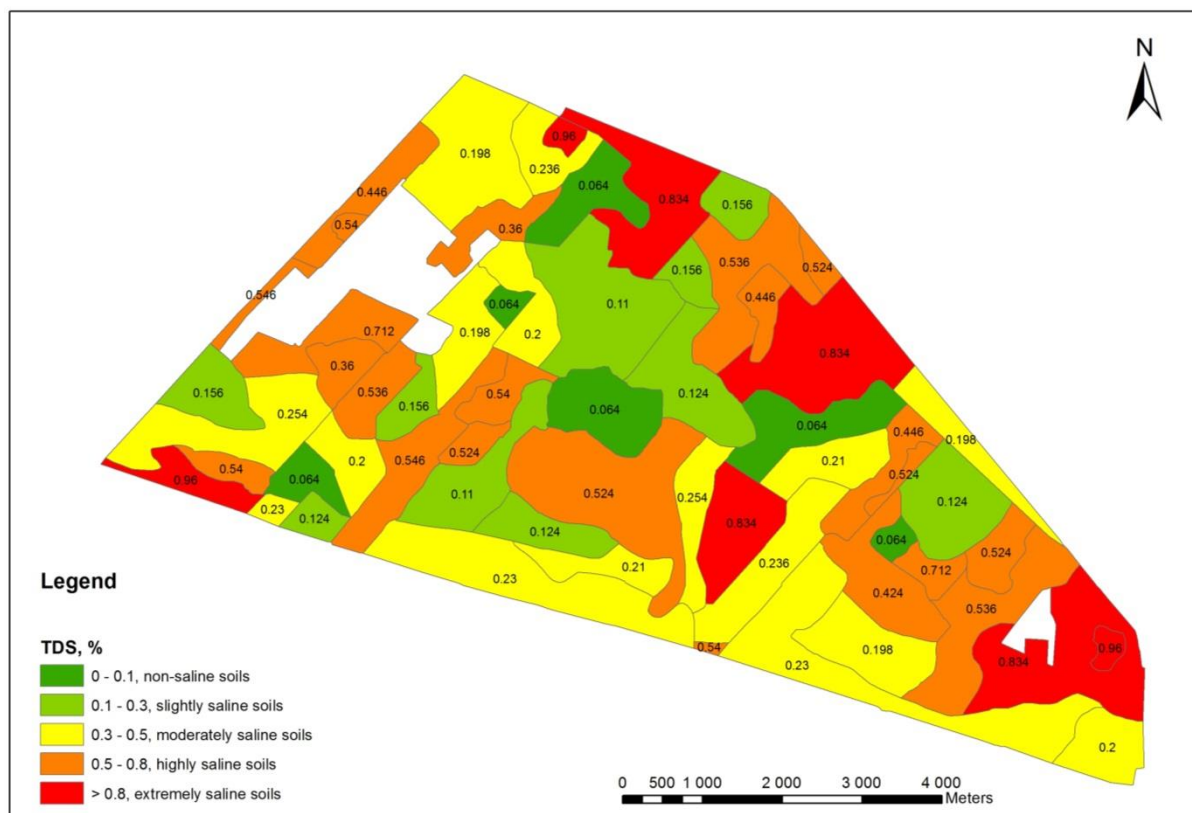
Figure 2. Soil salinity map of study area (digitised by author from map provided by State Research Institute of Soil Science and Agrochemistry)

2.3 Soil sampling and laboratory analysis

Four test fields on Bobur WUA were chosen. Soil samples were taken from the surface horizon (0-20 cm), since most of the researchers used this method (Aldakheel et al. 2006; Bannari et al. 2007; Bouaziz et al. 2011; Dutkiewicz et al. 2009; Eddine et al. 2012; Gutierrez and Johnson 2010; Noroozi et al. 2012; Sanaeinejad et al. 2009; Weng et al. 2010; Wu et al. 2008). In total thirty samples were taken from four different fields following simple random sampling technique.

Figure 3. Soil sampling points (October 2013)

After analysis of the results from the first sampling in October 2013 it was decided that additional sampling with some changes in sampling methods are necessary. For this reason second sampling session in March 2014 was organised (Figure 4). There were two main changes in methods: samples were

better distributed around the farm (7 fields were sampled), and soil was taken from 0-5 cm layer.
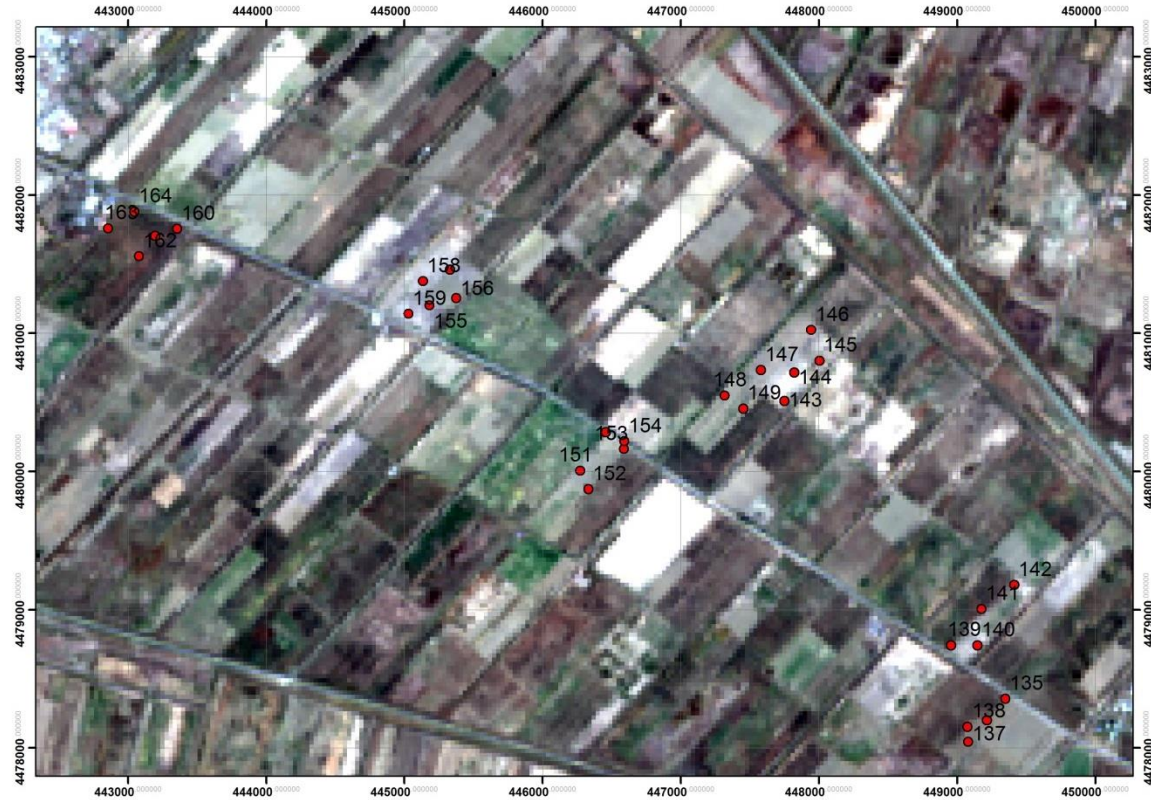
Figure 4. Soil sampling points (March 2014)

Soil samples have been air dried for several days. Then they were milled and sieved through a sieve with round holes of 1 mm size.

To prepare the aqueous extract, soil samples was weighted with an accuracy of 0.1 g and placed in to conical flask. Then distilled water has been added in proportion 1:5, one part of soil and five parts of water. Soil and water were stirred for 3 minutes.

2.3.1 Total dissolved salts content measurement using evaporation method

Then into funnels double folded filters were placed. Edge of a filter should be located 0.5-1 cm below the edge of a funnel. Slurry jet needs to be directed to the side wall of a funnel, to avoid tearing of a filter.

After filtering, 25 ml of filtrate was placed in a dried and weighed with an accuracy of 0.001 g porcelain cup and putted on water bath for evaporation. After evaporation cup was placed into thermostat and kept therein for 3 hours at 105 °C, cooled in desiccator and weighed with an accuracy of 0.001 g.

After that TDS in percent was calculated according to the formula:

$$X = \frac{(m - m1) * 500}{25},$$

where m – mass of a cup after evaporation, g;

m1 – mass of an empty cup, g;

500 – coefficient for percent recalculation (since extract was done in proportion 1:5);

25 – amount of extract taken for evaporation, ml.

2.3.2 Measuring of electrical conductivity of aqueous extract

For measuring conductivity Eijkelkamp 18.28 multimeter was used. To measure EC conductivity sensor should be immersed into aqueous extract and electrical conductivity can be determined. After each determination, sensor was washed with distilled water. Also before a measurement it is highly recommended to calibrate sensor, using 0.01 M KCl solution. Calibration procedure very simple. Electrode should was immersed into the calibration solution, together with the temperature electrode. Then, after 10 seconds, measurements were checked. The standard value for this solution is 1.41 mS. If numbers deviated from this value then calibration procedure was performed again.

In addition to this research, calibration curve for this device was drawn, to check the accuracy of the device. Five solutions of KCl were used, with concentration of 0.1M, 0.01M, 0.001M, 0.0001M, and 0.00001M. Next graph was received (Figure 5); R^2 value is close to 1. This test showed that the device gives reliable data and can be used during the research.
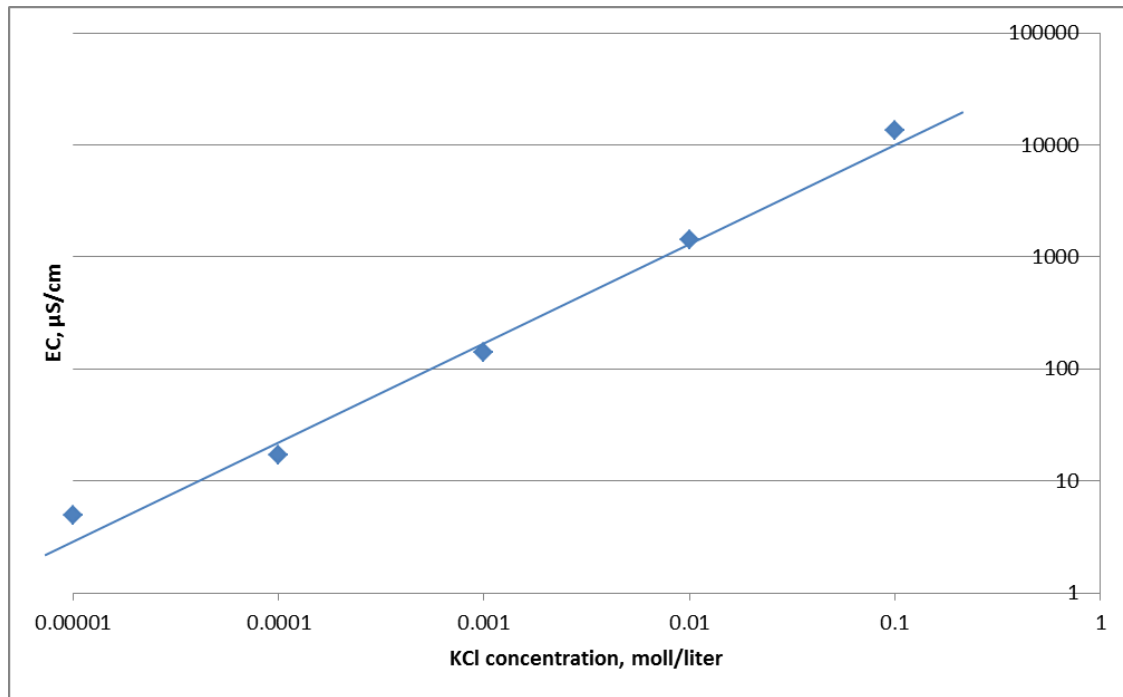
Figure 5. Calibration graph of Eijkelkamp 18.28 multimeter (logarithmic scale)

2.4 Comparison of TDS and EC values

To check how good EC measurements of Eijkelkamp 18.28 Multimeter correlate with more reliable measurements of total dissolved salts content, done by evaporation method, correlation analysis implemented. Obtained results (Figure 6) show R^2 of 0.92.
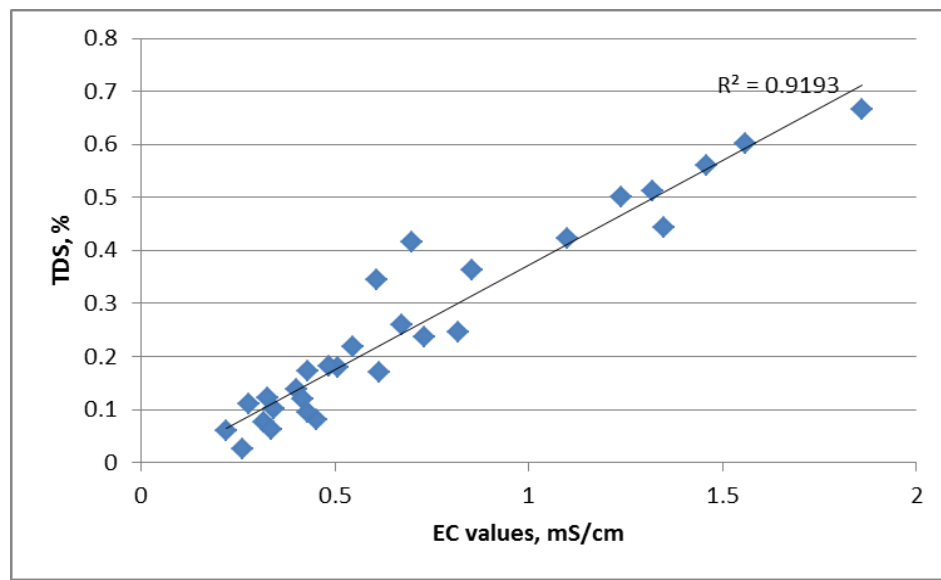
Figure 6. Scatterplot of TDS and EC values

This test also was implemented to use in future research only EC values and check how these values relate to TDS in soils of Syrdarya province. Since we observe mostly 100% correlation only EC values will be used in the rest part of the report, excluding secondary data.

To separate samples according FAO classification, multiplication coefficient from Watling (2007) were used. Values of $EC_{1:5}$ were multiplied by 9 and then classes showed in Table 2 were used.

Table 2. FAO classification of soil salinity based on EC_e

Salinity class	Non-saline	Slightly	Moderately	Very	Extremely
EC, ds/m	<2	2-4	4-8	8-16	>16

2.5 Landsat 8 sensor specifications

The Landsat 8 launched from Vandenberg Air Force Base in California on February 11, 2013, atop an Atlas V rocket. As with previous partnerships, this collaboration between the U.S. Geological Survey (USGS) and National Aeronautics and Space Administration (NASA) continues the mission to acquire high-quality data that meet both USGS and NASA scientific and operational requirements for observing land use and land cover change. The Landsat era that began in 1972, providing global, synoptic, and repetitive coverage of the Earth's land surfaces, continues at a scale where natural and human-induced changes can be detected, differentiated, characterized, and monitored over time.

The Landsat 8 spacecraft, built by Orbital Sciences Corporation, has a 5-year mission design life, yet includes enough fuel for 10 years of operation. The centrepiece of the observatory is the Operational Land Imager (OLI), which was designed and built by the Ball Aerospace and Technologies Corporation. By collecting land-surface data with spatial resolution and spectral band specifications consistent with historical Landsat data, the OLI instrument advances future measurement capabilities while ensuring compatibility with historical data.

Designed as a push-broom sensor with a four-mirror telescope, higher signal-to-noise performance, and 12-bit quantization, the OLI collects data in the visible, near infrared, and shortwave infrared wavelength regions as well as a panchromatic band. Two new spectral bands have been added: a deep-blue band for coastal water and aerosol studies (band 1), and a band for cirrus cloud detection (band 9) (Figure 7). A Quality Assurance band is also included to indicate the presence of terrain shadowing, data artefacts, and clouds (USGS 2013).
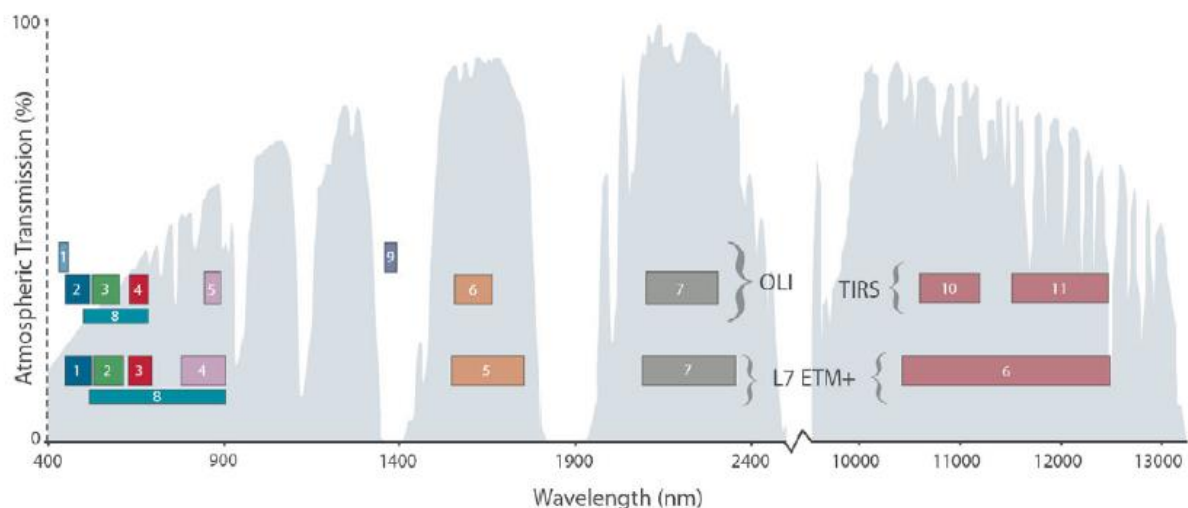
Figure 7. Band passes of the Landsat 8 Operational Land Imager (OLI) and Thermal Infrared Sensor (TIRS) instruments (USGS 2013).

Table 3. Processing parameters for Landsat 8 standard data products (USGS 2013).

[UTM, Universal Transverse Mecator; WGS, World Geodetic System; OLI, Operational Land Imager; TIRS, Thermal Infrared Sensor]

Product Type	Level 1T (terrain corrected)
Data type	16-bit unsigned integer
Output format	GeoTIFF
Pixel size	15 meters/30 meters/100 meters (panchromatic/multispectral/thermal)
Map projection	UTM (Polar Stereographic for Antarctica)
Datum	WGS 84
Orientation	North-up (map)
Resampling	Cubic convolution
Accuracy	OLI: 12 meters circular error, 90 percent confidence TIRS: 41 meters circular error, 90 percent confidence

2.6 Image pre-processing

Study area characterised by more than 300 sunny days in a year, so the only pre-processing done is conversion of the recorded Digital Numbers to top of the atmosphere (TOA) reflectance. This procedure was done according to guidelines of USGS (http://landsat.usgs.gov/Landsat8_Using_Product.php), details of which can be found below.

Conversion to TOA Reflectance

OLI band data can also be converted to TOA planetary reflectance using reflectance rescaling coefficients provided in the product metadata file (MTL file). The following equation is used to convert DN values to TOA reflectance for OLI data as follows:

$$\rho\lambda' = M_\rho Q_{cal} + A_\rho$$

where:

$\rho\lambda'$ = TOA planetary reflectance, without correction for solar angle. Note that $\rho\lambda'$ does not contain a correction for the sun angle.

M_ρ = Band-specific multiplicative rescaling factor from the metadata (REFLECTANCE_MULT_BAND_x, where x is the band number)

A_ρ = Band-specific additive rescaling factor from the metadata (REFLECTANCE_ADD_BAND_x, where x is the band number)

Q_{cal} = Quantized and calibrated standard product pixel values (DN)

 TOA reflectance with a correction for the sun angle is then:

$$\rho\lambda = \frac{\rho\lambda'}{\cos(\theta_{SZ})} = \frac{\rho\lambda'}{\sin(\theta_{SE})}$$

where:

$\rho\lambda$ = TOA planetary reflectance

θ_{SE} = Local sun elevation angle. The scene center sun elevation angle in degrees is provided in the metadata (SUN_ELEVATION).

θ_{SZ} = Local solar zenith angle; $\theta_{SZ} = 90° - \theta_{SE}$

For more accurate reflectance calculations, per pixel solar angles could be used instead of the scene center solar angle, but per pixel solar zenith angles are not currently provided with the Landsat 8 products.

 Conversion to At-Satellite Brightness Temperature

TIRS band data can be converted from spectral radiance to brightness temperature using the thermal constants provided in the metadata file:

$$T = \frac{K_2}{ln(\frac{K_1}{L_\lambda} + 1)}$$

where:

T = At-satellite brightness temperature (K)

L_λ = TOA spectral radiance (Watts/(m2 * srad * µm))

K_1 = Band-specific thermal conversion constant from the metadata (K1_CONSTANT_BAND_x, where x is the band number, 10 or 11)

K_2 = Band-specific thermal conversion constant from the metadata (K2_CONSTANT_BAND_x, where x is the band number, 10 or 11)

2.7 Image analysis

For image analysis two software packages were used – Erdas Imagine and ArcGIS.

Images were downloaded from Earthexplorer USGS web-site. Images for three dates were used – 30th August 2009 (for secondary data), 5th May and 28th October 2013. Path and Row of the downloaded images are 154 and 032 respectively. After downloading all bands of the image were opened as a Virtual Stack in Erdas and then Subset Image of the study area was created. All next manipulations were performed on this Subset image in .img format.

All tested indices were calculated using Erdas modeller. For all indices it was a one-step procedure (Figure 8). After calculations an index values for specific ground truth points were extracted into one table, using ArcGIS tool named Extract Multi Values to Points.

For secondary data analysis methods were different (Figure 9). First two masks based on
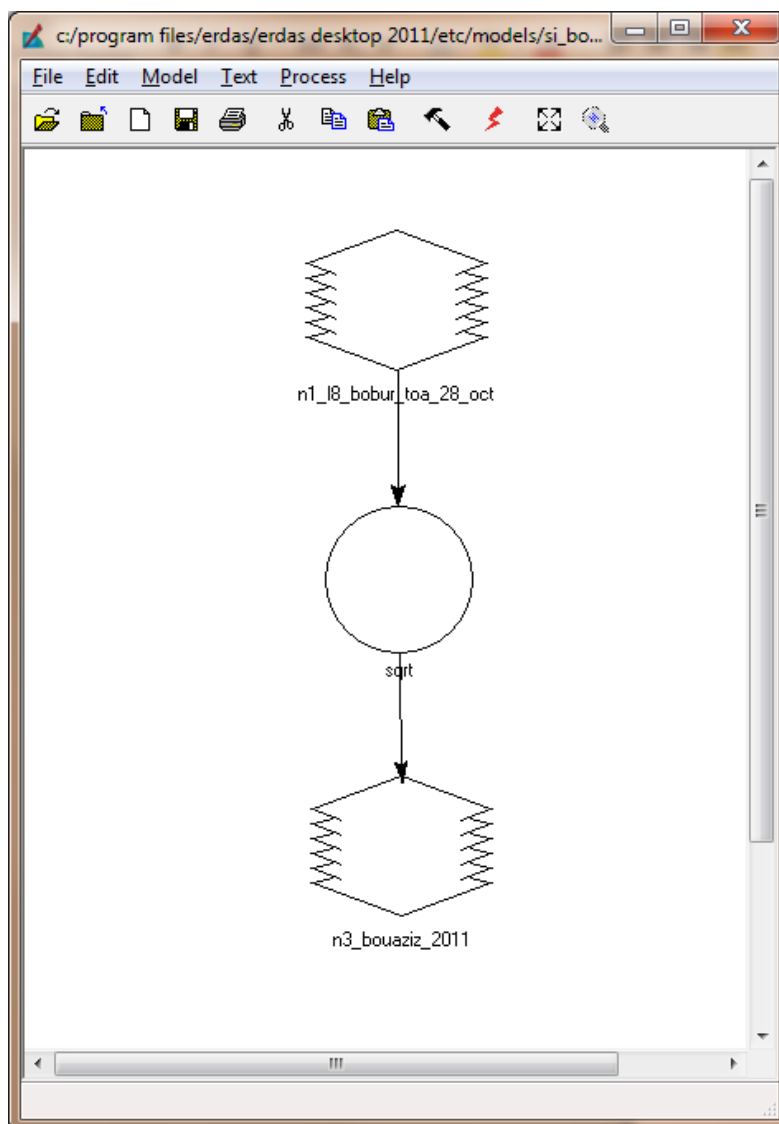
Figure 8. Example of model for index calculation
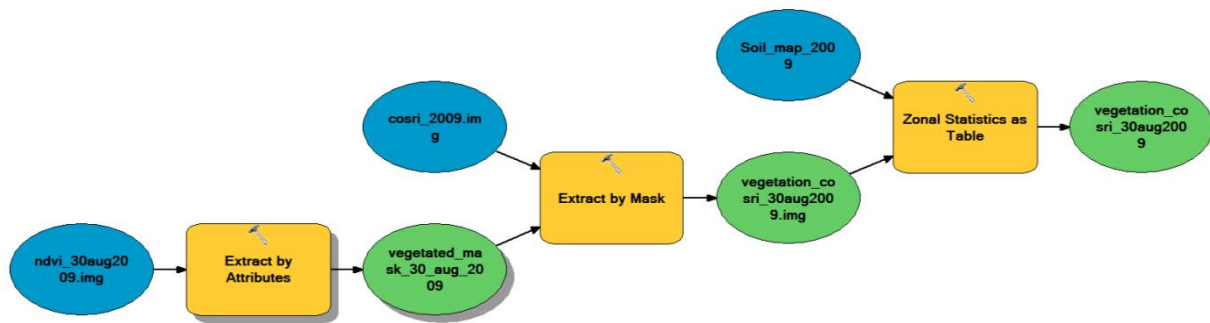
Figure 9. ArcGIS model for secondary data analysis

NDVI values were created for study area. This was done to separate bare soil areas and areas covered by vegetation. It was necessary because both indices for bare soil and for vegetation were tested. After that values for each index were extracted by masks, COSRI by mask for vegetated area and all other indices using mask for bare soil. Then the average value for every index per zone was calculated in ArcGIS using tool Zonal Statistics as Table. After that tables were imported into Microsoft Excel for statistical analysis.

3. Results and discussion

Following the methods described in the previous section next results were obtained.

In total 30 samples were collected on four fields, three bare fields and one field with cotton during the first sampling session. Samples from cotton covered fields were excluded at the beginning, since it was planned to compare this samples with vegetation reflectance in august, but soon it was discovered that it not possible to combine vegetation indices values for different crops (bare fields before were covered by wheat). Also it wasn't useful for bare soil indices analysis since it was covered by cotton plants. So data from 25 samples was included into analysis.

Between these three fields, field 2 tends to have most equally distributed samples in sense of salinity classes. In samples from field 1 very saline soils prevail, in field 3 slightly saline soils prevail (Figure 10).
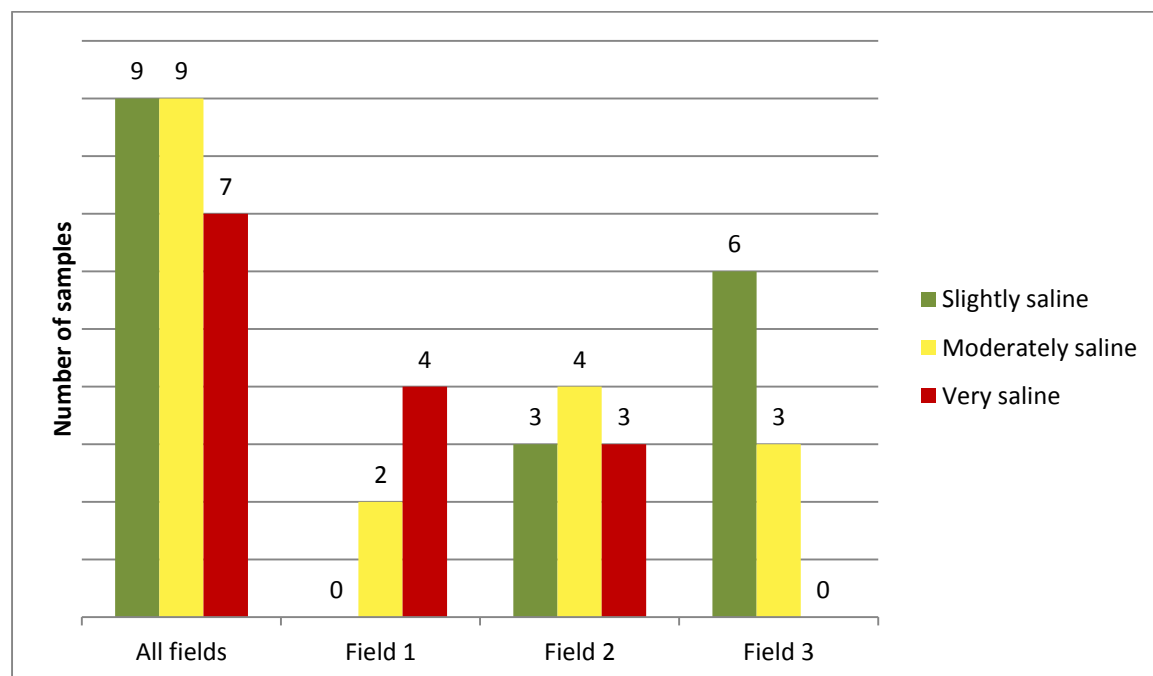
Figure 10. Distribution of samples per field and salinity class

3.1 Testing of existing indices

3.1.1 Indices tested on bare ground
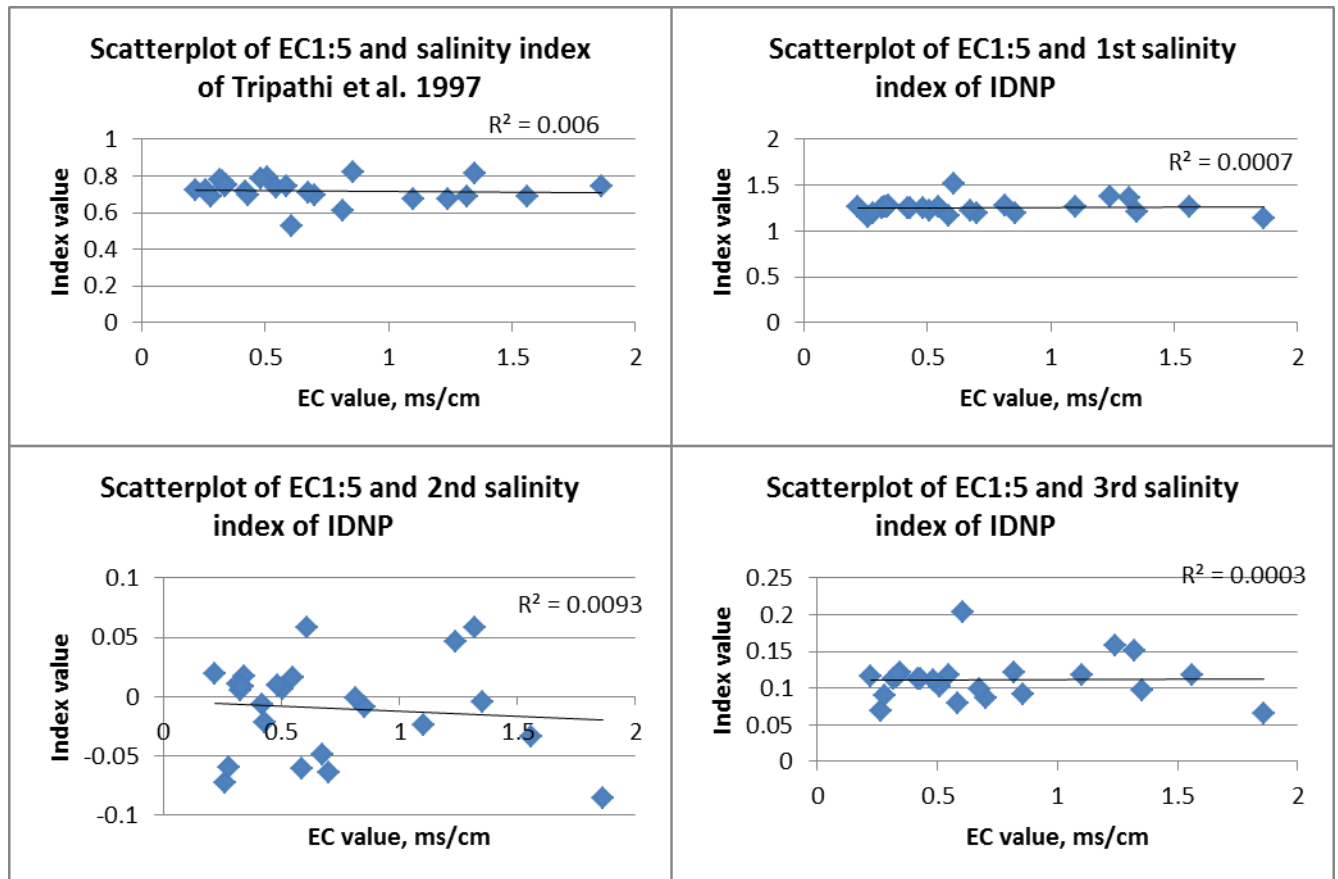
Figure 11. Scatterplots of indices versus EC values for IDNP indices and index from Tripathi et al. 1997 (hereinafter indices formulas and numbering as in Table 1)

As can be seen from the graphs in Figure 11, none of the IDNP indices shows significant correlation. In Indo-Dutch Network Project (2002) authors did not mention exact correlation values but it is clear that correlation was significant, since these indices were used for further classification in their work. To understand why in Syrdarya region these indices shows such a low correlation we decide to analyse differences in study area, including climate, soil and other factors that can influence results. According to Indo-Dutch Network Project (2002) their research was implemented in the Bhalaut distributary command, India. This study area falls in semi-arid region with an average annual rainfall of 545 mm and average annual evapotranspiration of 1650 mm. The average

minimum and maximum temperature fluctuates between 5-45 C°, respectively. The soil is mainly alluvium, light textured categorised as sandy loam to loamy sand. So both this study area and Syrdarya province falls in semi-arid region, precipitation levels are also comparable, soil texture in both case loam, sandy loam. Soil salinity varies between 0-12 ds/m (non-saline to highly saline). So according to this parameters two study areas are comparable. Of course satellite images were produced by different sensors (Landsat 5 in case of IDNP and Landsat 8 in case of this research) but this shouldn't influence results since NASA and USGS mentioned many times that Landsat sensors are created as follow ups and all images are comparable to each other, despite small differences in bands width.

But in report of IDNP exact information about the soil type is not mentioned and this can be the reason of differences. It is known that soil cover in Syrdarya region is presented by grey-meadow, meadow and light grey soils (Goskomgeodezkadastr 2010).
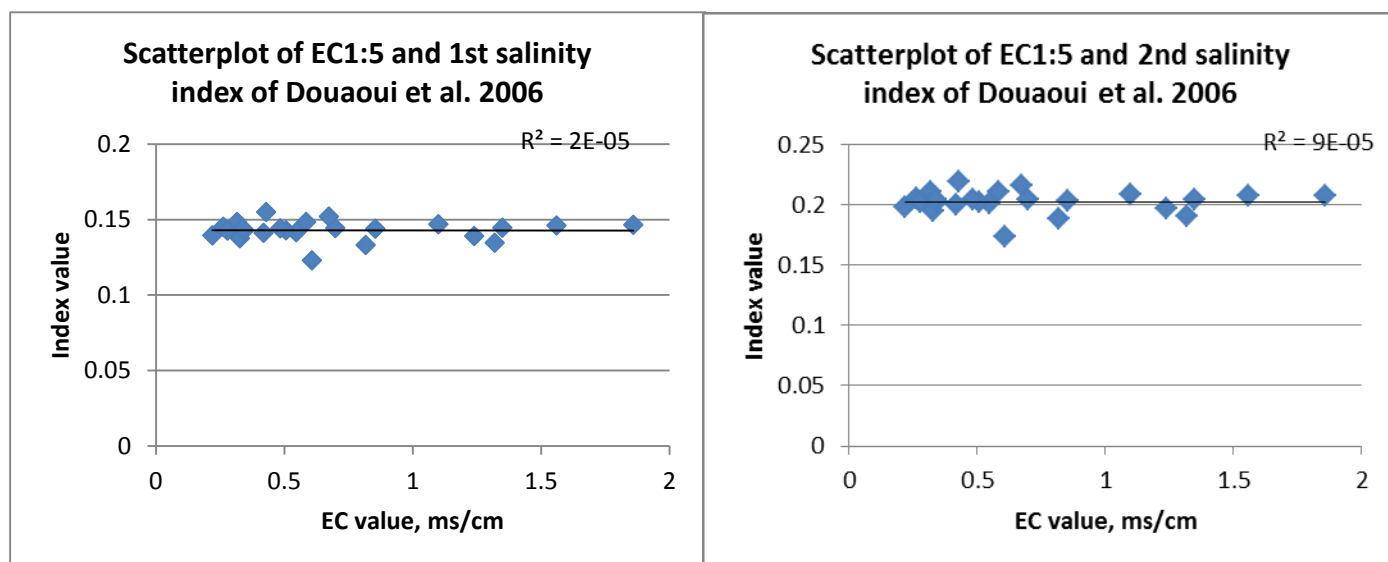

Figure 12. Scatterplots of indices values of Douaoui et al. 2006

Next two indices for testing were indices presented in work of Douaoui et al. (2006). In the work of Douaoui et al. (2006) these indices showed correlation coefficient values 0.50 and 0.49 but in the current study the correlation is again

not significant (Figure 12). The study areas is again, as in previous case are comparable. Lower Chéliff Plain in Northwest Algeria also falls into semi-arid climatic zone, with precipitation level of 250 mm per year. There is some data about soils available in that work. Mentioned that soils in that area are limey and with clayey texture, which means that soils here also similar by its properties to the soils of Syrdarya region. Salinity varies from 0 to 60 ds/m (non-saline to extremely saline), this range are much broader than a range in our case – 1.5 to 16 (non-saline to highly saline). Differences in sensors also could lead to differences in results. Douaoui et al. (2006) used images of SPOT XS sensor. If compared with Landsat 8 we can say that bands of Landsat little bit narrow. Green band in Landsat 8 – 60 nm wide, in SPOT XS – 90 nm, red band 30 and 70 nm, and NIR band 30 and 100 nm wide respectively. Difference can be considered significant but it is hard to say how big the influence of this to the end result.

One more big difference is the number of samples. In work of Douaoui et al. (2006) they used more than 3980 samples, in case of this research the number was much lower.

Bouaziz et al. (2011) reported in their work that above mentioned index shows a correlation of 0.58 with EC values in their research in Brazil. But on test site of Syrdarya province values were much lower, close to 0 (Figure 13). But also important that in work of Bouaziz et al. (2011) linear spectral unmixing technique was applied. The correlation coefficient without this technique was lower, around 0.4, but it is still much higher than in current research. This can lead to the idea that something else can cause this difference.
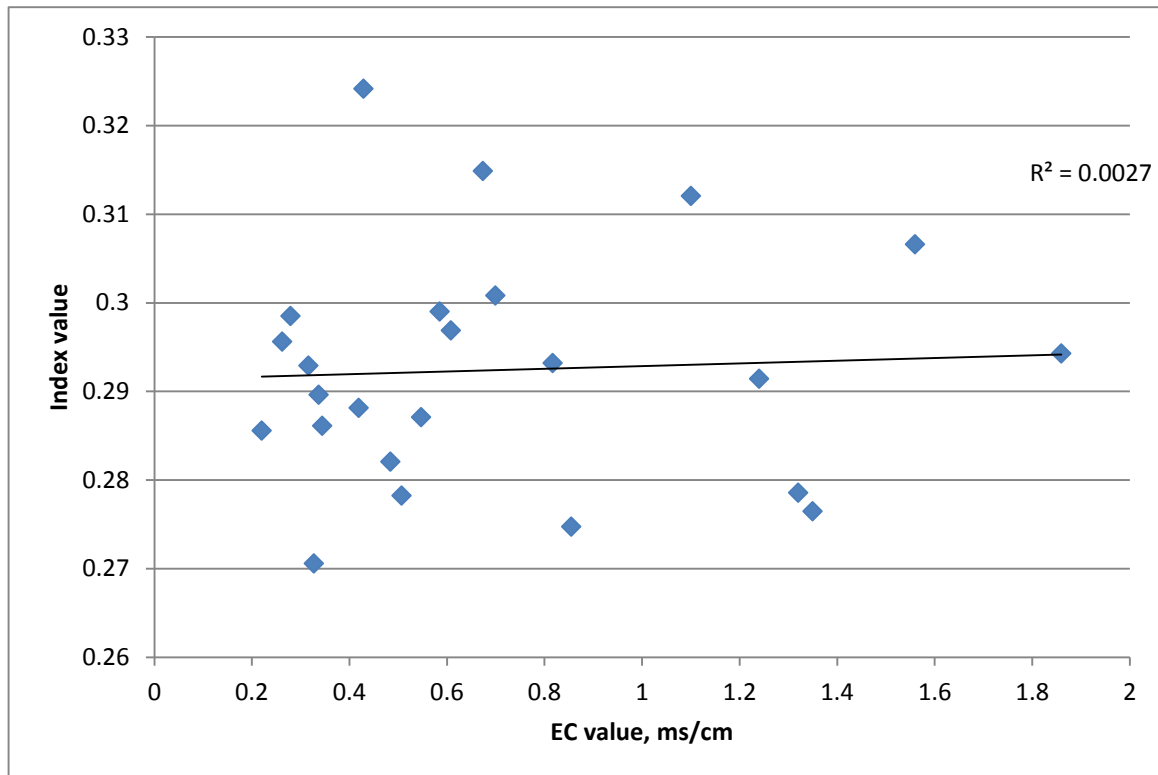
Figure 13. Scatterplot of EC1:5 and 1st salinity index of Bouaziz et al. 2011

Again the use of different sensors can contribute to these results. Bouaziz et al. (2011) used MODIS images, but spectral difference are not so critical here, most of the used bands are a little bit broader on Landsat sensor, but only for few nm. The difference in optical resolution are more significant – pixel size of MODIS 250 m and for Landsat 30 m. There is no precise data on soil in that work, but it is most likely that soils in Brazil will differ dramatically from soils of Uzbekistan. Also important that on image provided in their article we can see that most of the study area covered by vegetation and, since MODIS have relatively big pixel size, some vegetation reflectance can be captured on these images, but in case of our work fields were free of any vegetation.

Four indices from the work of Abbas et al. (2013) also showed no significant correlation, including fourth index, which showed highest correlation (0.7-0.8) during above mentioned research (Figure 14). Study area in this research was located in Pakistan, area characterised by authors as semi-arid, with low

precipitation, soils are mainly alluvial deposits, the same as in Syrdarya
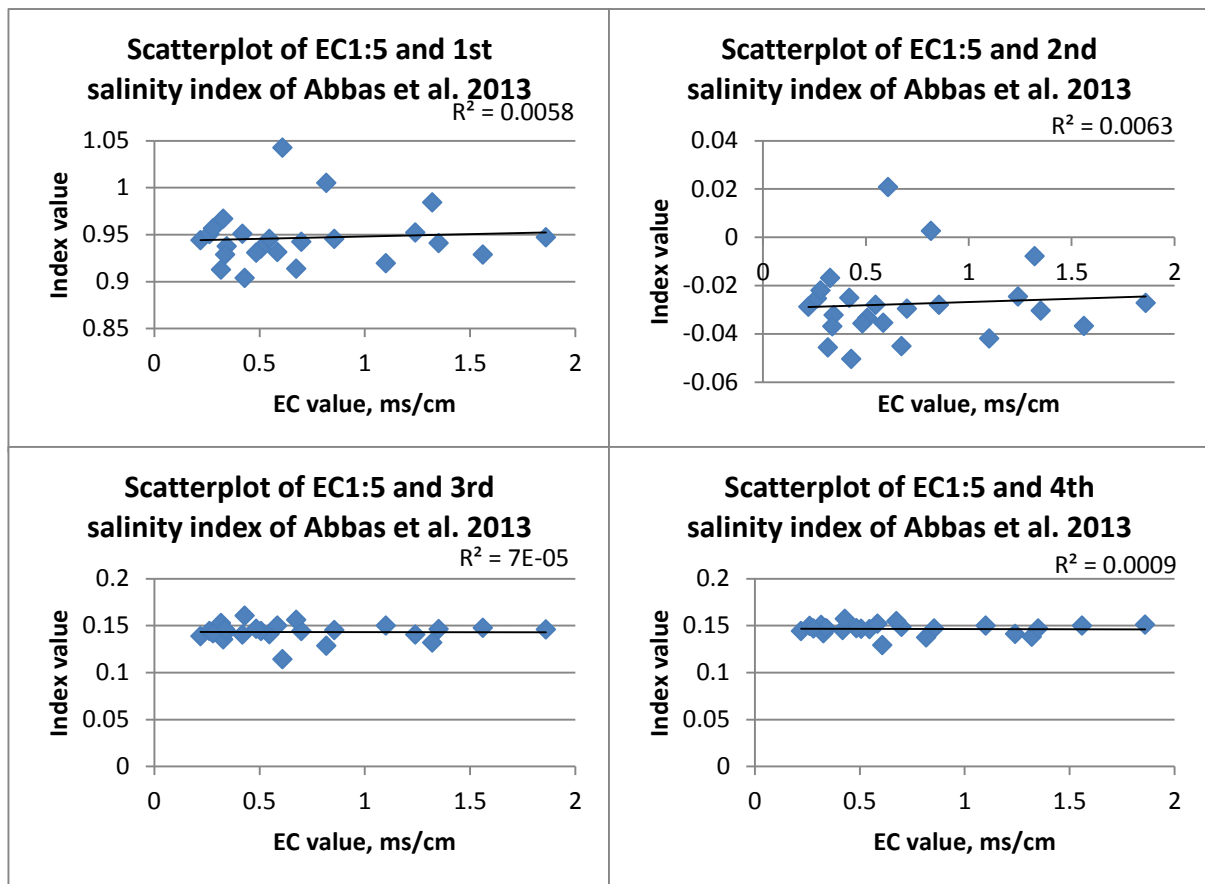
Figure 14. Scatterplots of EC and salinity index of Abbas et al. 2013

province. Salinity varies in a range 0-23 ds/m.

Images used were pictured by IRS-1B LISS-II satellite. Spectral properties differ from Landsat (Table 4). Especially big difference between two sensors can be observed in NIR band.

Table 4. Characteristics of the images used in work of Abbas et al. (2013)

Band	Spectral range (µm)	Spatial resolution (m)
1	0.45–0.52	36.25
2	0.52–0.59	36.25
3	0.62–0.68	36.25
4	0.77–0.86	36.25

So in this case differences in sensors and soil type can be the reason of the unsatisfactory results.

3.1.2 Testing of vegetation indices
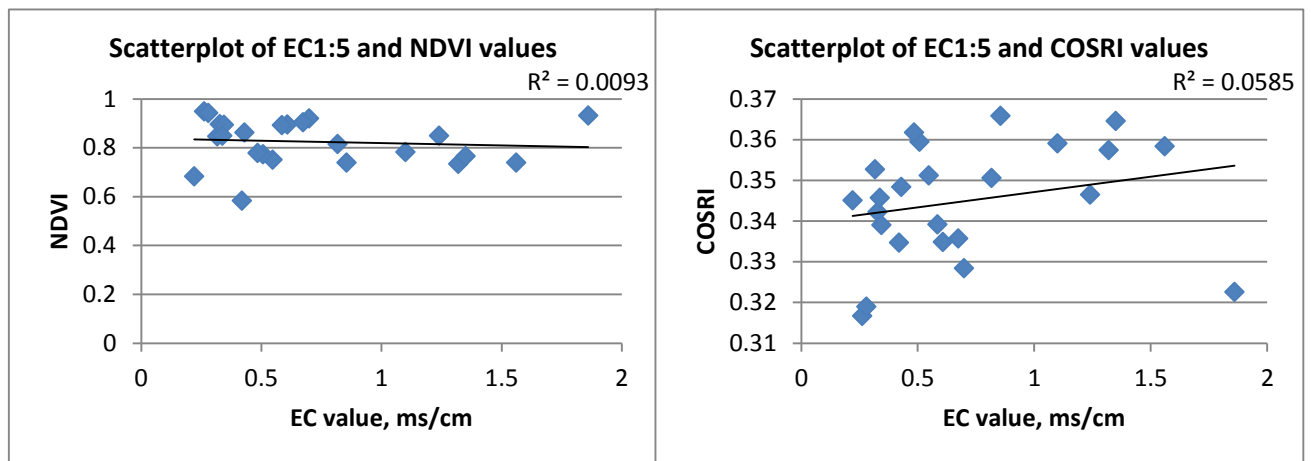
Figure 15. Scatterplot of NDVI and COSRI versus EC

In addition to bare soil indices, indices that used vegetation as a proxy parameter were calculated for study area.

The well-known normalised vegetation index (NDVI) was calculated but showed no significant correlation in our case (Figure 15). Reason could be the big time span between the sampling date (October 24th) and the date of image acquisition (5th May), used in analysis.

But the second index COSRI performed much better. This index also involving NDVI into calculation and formulated as COSRI = [(band 2 + band 3)/(band 4 + band 5)]*NDVI for Landsat 8 data.

Table 5. Correlation coefficients table for COSRI index

Field ID	Correlation coefficient (R)	Correlation coefficient (R) (without one outlier point)
All fields	0.24	0.53
Field 1	0.52	0.52
Field 2	0.32	0.79
Field 3	0.49	0.49

Correlation coefficient for all three fields 0.06, but if you look to coefficients for individual fields you can see that values are much higher (Table 5). In case of the field two the reason could be the outlier point.

R^2 value that showed Fernández-Buces et al. (2006) was higher, they report $R^2=0.83$. But during their processing they used correction for mixed pixels, which contained from different plant species. Ground radiance was obtained for each plant species (FOV of 0.385m2), COSRI was calculated for each species and multiplied by their proportional participation value in each site. The resulting values for all of the plant species present were finally added. These resulted in a weighted representative COSRI assigned to each pixel with mixed plant constituents, and was used as spectral response indicator for each site. Since our test sites contained only one plant species no such correction was done.

Field 2 was a field with a highest variance in soil salinity level; samples from this field represent slightly saline, moderately saline and highly saline areas. And correlation coefficient of 0.79 on this field for COSRI shows potential of this index for salinity assessment on this area.

3.2 Reflectance of individual bands

Correlation analysis of individual reflective bands was implemented.

Table 6. Correlation coefficients (R) for individual Landsat 8 bands reflectance with EC values (bare soil)

Field ID	band 1	band 2	band 3	band 4	band 5	band 6	band 7
All fields	0.10	0.00	0.05	-0.05	0.06	0.11	0.09
Field 1	0.50	0.46	0.62	0.56	- 0.53	- 0.75	- 0.13
Field 2	- 0.08	- 0.06	- 0.11	- 0.02	- 0.14	- 0.11	- 0.09
Field 2 (without outlier)	-0.30	-0.28	-0.18	-0.06	0.33	-0.28	-0.59
Field 3	0.42	0.26	0.16	0.08	- 0.23	- 0.12	- 0.01

None of the bands shows significant correlation if take into account all three fields. Field one shows some correlation, but these results cannot be reliable because of the small number of points in field 1.

Highest correlation can be observed for band 1, 6 and 7.

Despite higher correlation levels for the individual field we did not consider these results persistent and do not develop further discussion in this vein.

3.3 Spectral signatures analysis
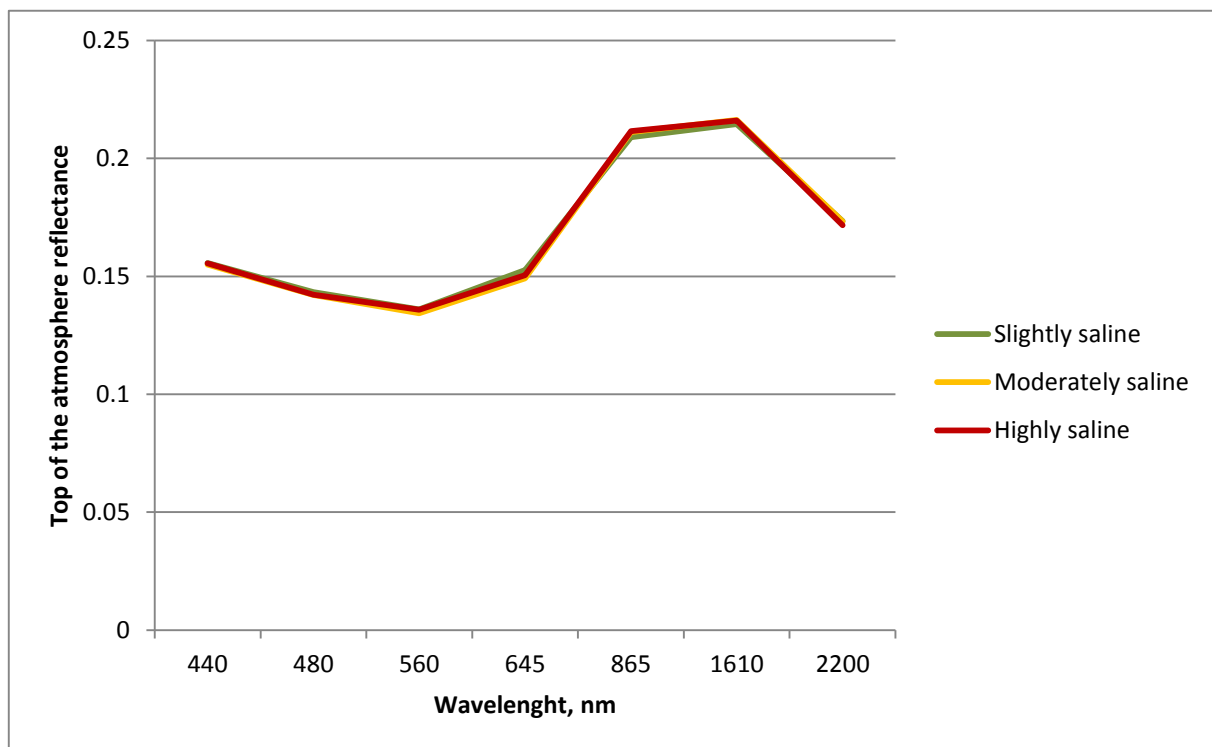
Figure 16. Averaged spectral signatures of soils in Syrdarya region with different salinity levels

Soil spectra per salinity class were averaged and graph plotted (Figure 16). No difference can be observed in spectral reflectance of soils between salinity classes.
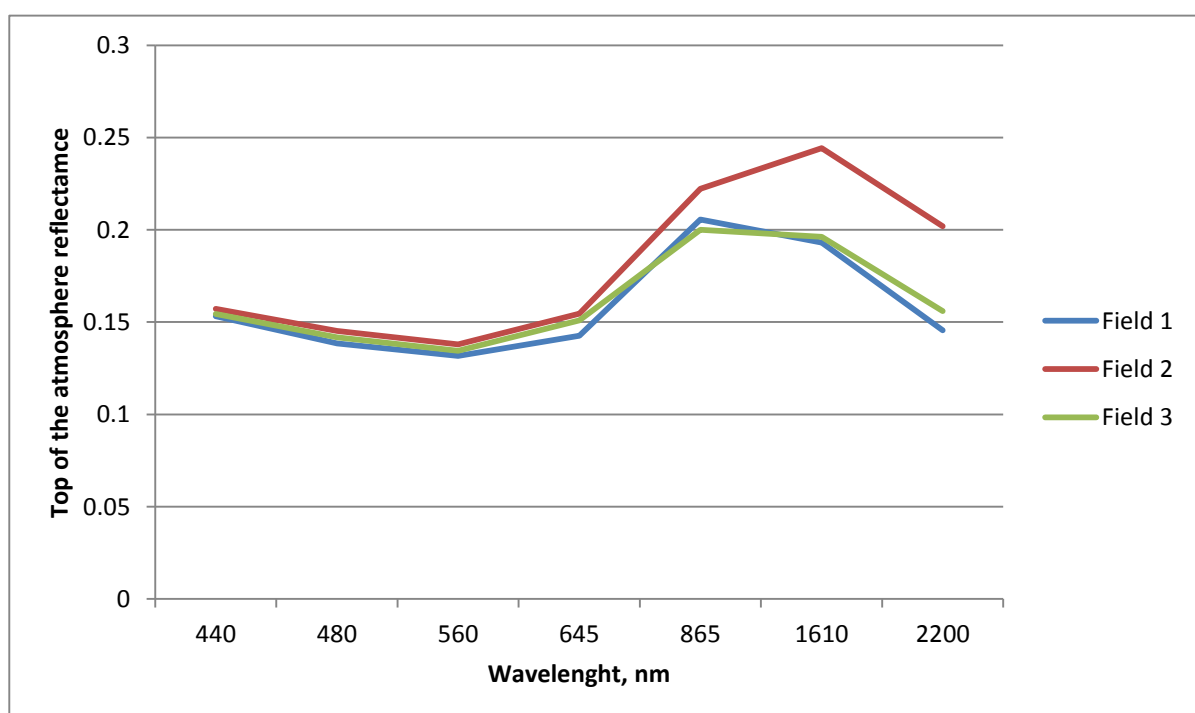
Figure 17. Averaged spectral signatures of soils in Syrdarya region for three test fields

Also averaged spectra per field were plotted (Figure 17). Here difference of field 2 especially distinguishable. Reflectance in band 5, 6 and 7 (NIR and SWIR bands) are higher than on two other fields. One of the possible explanations of this differences is that field 2 was ploughed shortly before the date of image acquisition. And field 1 and 3 were not ploughed.
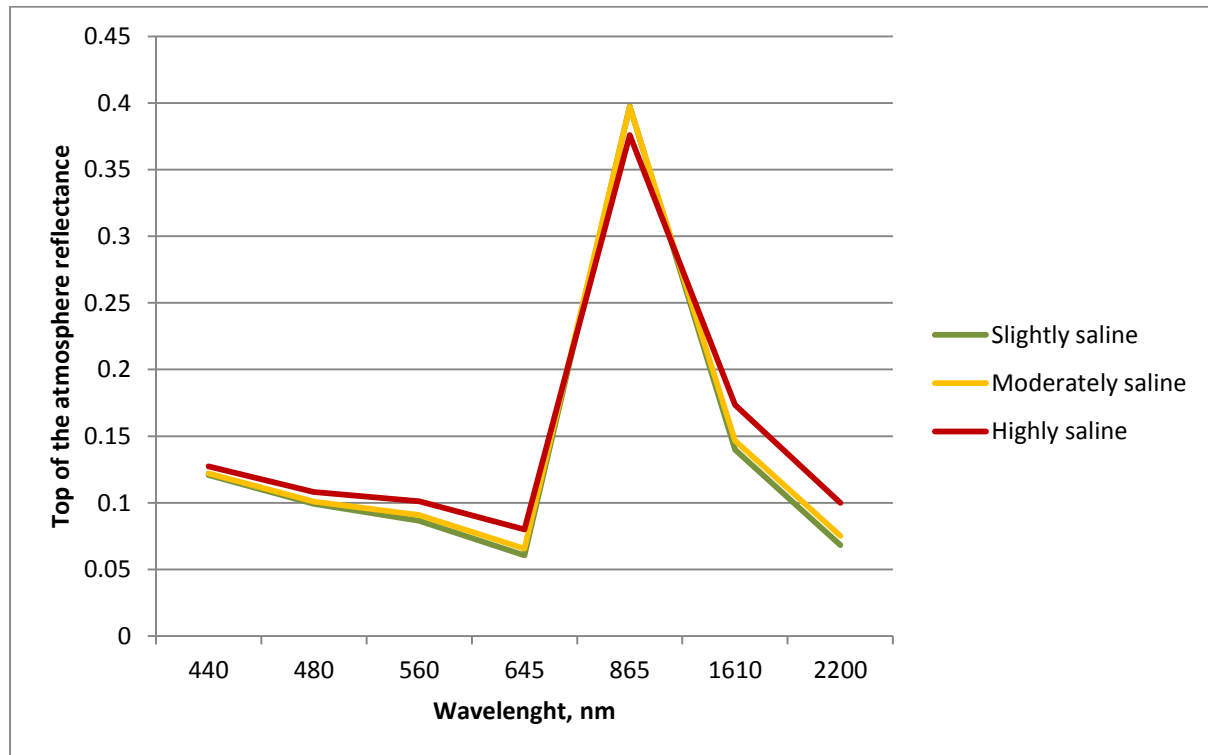
Figure 18. Averaged spectral signatures of vegetation in Syrdarya region with different salinity levels

A similar figure with spectral signatures was plotted for vegetation. Here the difference between salinity classes already can be seen, especially clearly distinguished higher reflectance and lowest NIR peak of vegetation on highly saline soils (Figure 18). But in NIR band we see some decrease if compared with other classes, which is a normal thing for suppressed vegetation (in this case by high salts content in soil). The difference between slightly and moderately saline signature is not so big, but also visible.
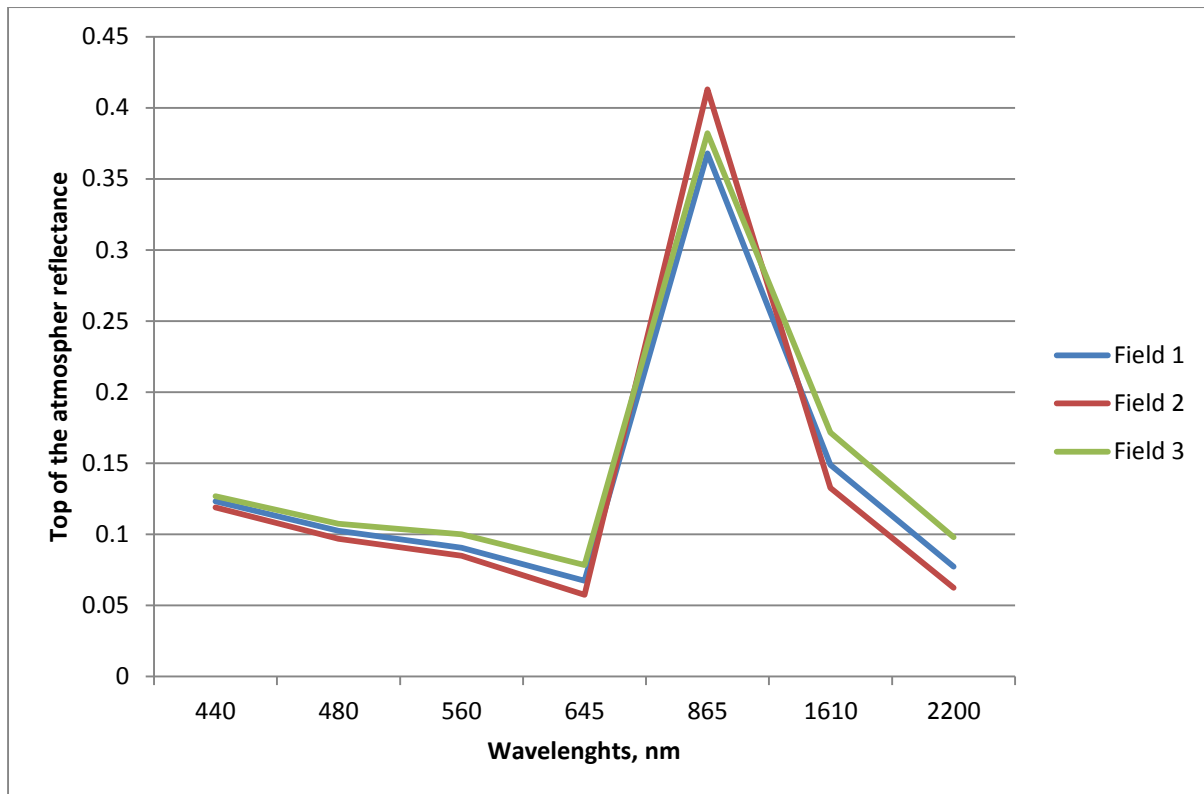
Figure 19. Averaged spectral signatures of vegetation in Syrdarya region for three test fields

A similar graph was plotted for different fields also (Figure 19). Here difference between fields is still present, but field two already not as different as on bare soil signatures graph (Figure 17).

3.4 Secondary data analysis

In addition to ground truth data collected during thesis we also analysed map of State Research Institute of Soil Science and Agrochemistry. Similar to the previous steps different soil indices were calculated. Next, the correlation coefficients between the soil salinity values and the soil indices were calculated (Table 7).

Table 7. Correlation coefficients (R) of bare soil indices, calculated based on secondary data

Index	Tripathi 1997	IDNP 2002 1	IDNP 2002 2	IDNP 2002 3	Douaoui 2006 1	Douaoui 2006 2	Bouaziz 2011	Abbas 2013 1	Abbas 2013 2	Abbas 2013 3	Abbas 2013 4
R	-0.13	-0.30	0.00	0.37	0.21	0.23	0.30	-0.40	-0.41	0.27	0.20

Here we can see that the values are higher than in the previous dataset. Especially higher correlation of first and second index of Abbas et al. (2013), with this dataset it reaches R values up to -0.41, which is still low for good prediction, but already close to it.
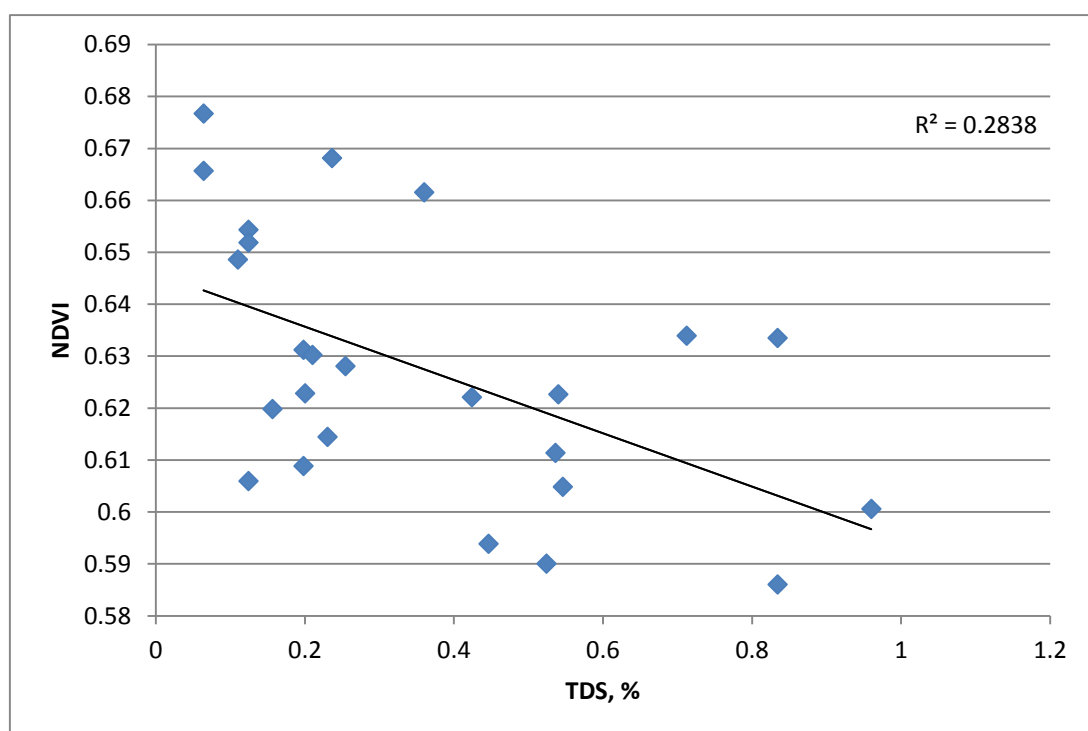
Figure 20. NDVI versus TDS scatterplot, based on secondary data (Soil research institute map)

R² = 0.3293
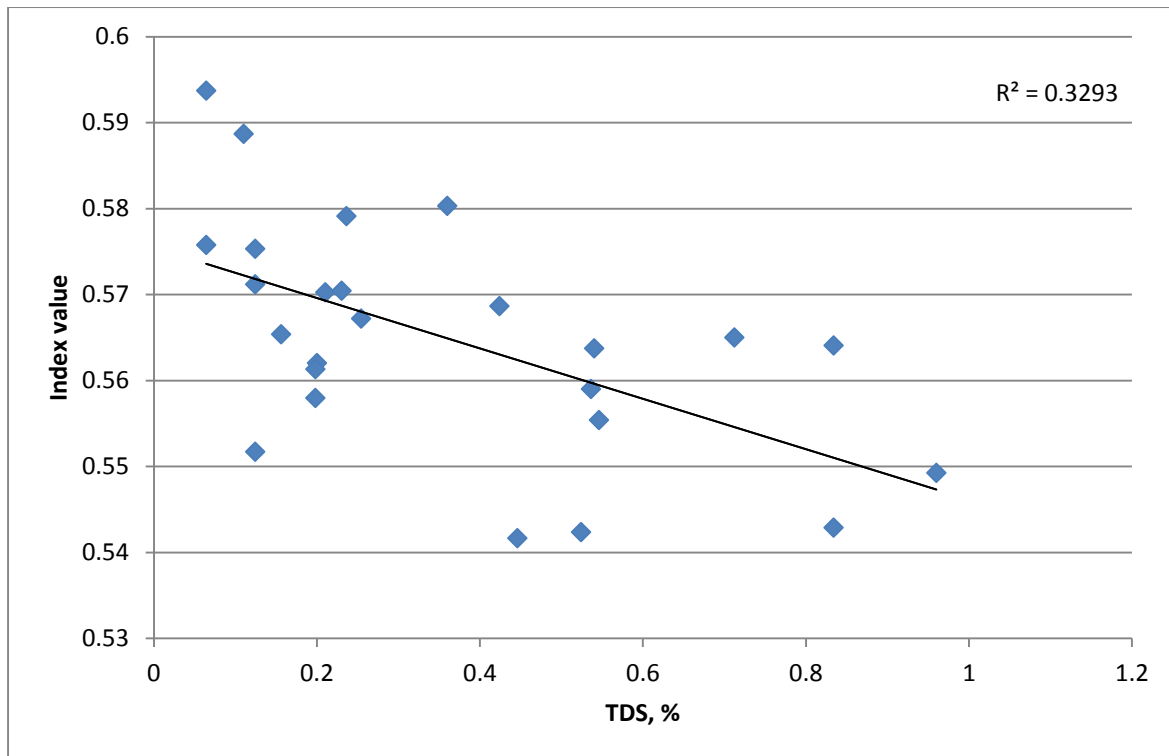
Figure 21. COSRI versus TDS scatterplot, based on secondary data (Soil research institute map)

Vegetation indices also performed better with this dataset, both NDVI and COSRI (Figure 20 and Figure 21). Highest achieved R value is -0.57 for COSRI, which is already significant.

There are several reasons that could lead to better calculation results with this secondary dataset. First of all this dataset can be considered as broader and it covers a much bigger area than only data that was collected specifically for this thesis. Also for this comparison we calculate average index values for each of 25 zones. This averaging could positively influence correlation values in comparison with calculation when values from individual pixels used.

Also we analysed spectral signatures for different salinity classes, same as in previous dataset (Figure 22). But difference here that we used spectra not from individual pixels and then averaged them, here we used averaged spectra for each zone, and then averaged between several zones of the same class of salinity. So here we can see so called double averaging. Reliability of these

results can be questioned because we not used pure spectra, but still this analysis can reveal some regularities and patterns.

For the governmental map dataset we can see difference in bare soil spectra (Figure 22) for the different salinity classes. It is seen that soils with higher salinity level shows higher reflectance in general, excluding moderately saline class, which showed lowest reflectance, even lower than reflectance for slightly saline class. This inconsistency might be caused by this double averaging and assumption that for each zone of map (the one we used as secondary data) salinity level will be the same, which is not true. So, on this graph (Figure 22) we see some possibilities to distinct between different salinity classes, but this inconsistency about moderately saline class shows that these results still not persistent.
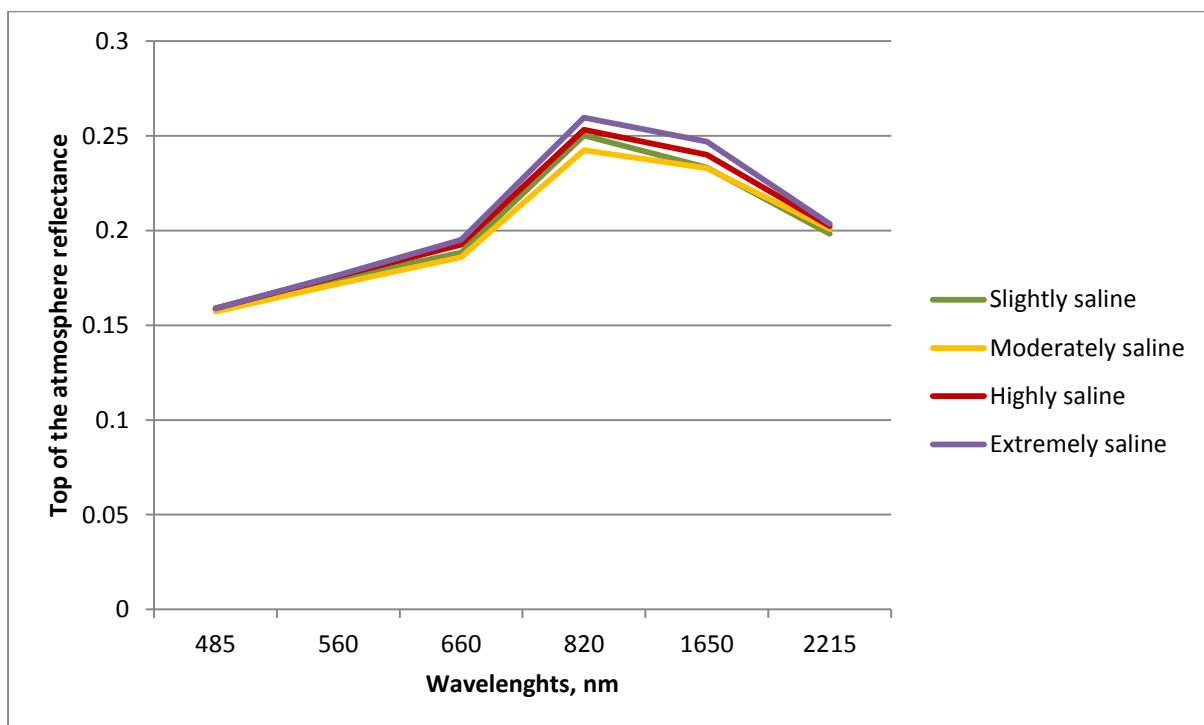
Figure 22. Averaged spectral signatures of soils in Syrdarya region with different salinity levels (secondary data)

Same signatures were plotted for vegetation reflectance also (Figure 23). Here differences are less visible, when compared with the bare soil dataset. But we

still can see highest NIR peak for slightly saline signature and lowest peak for extremely saline class. This less pronounceable difference could be the reason of crop diversity that we include into dataset when used secondary data. In secondary data we used averaged NDVI values between different crops that growth on area with one salinity level. But different crops are differently susceptible to soil salinity. So this result showed us that main trend (lower salinity – higher NIR peak and lower red peak) still present can and it was confirmed in both datasets, despite that for the vegetated images the difference is less pronounced.
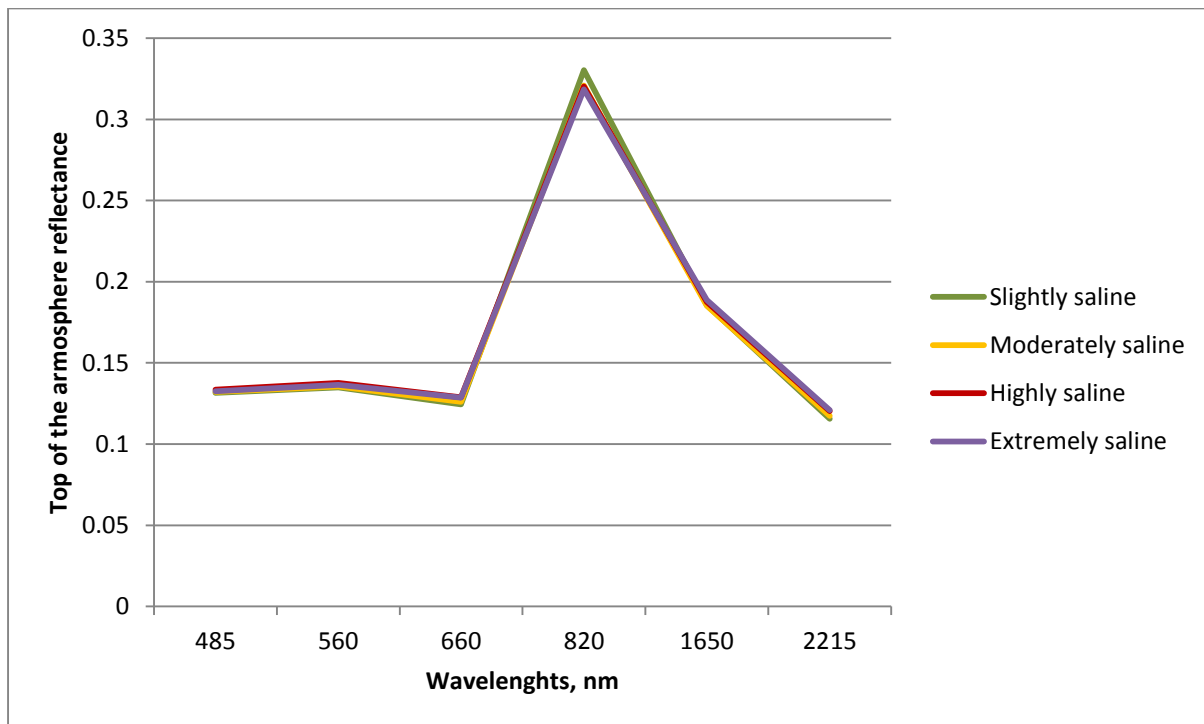
Figure 23. Averaged spectral signatures of vegetation in Syrdarya region with different salinity levels (secondary data)

3.5 Results of the second sampling

To confirm previous results second sampling session was organised with some changes in methods which were mentioned in Materials and methods section. Next graphs and tables represent all data analysed.
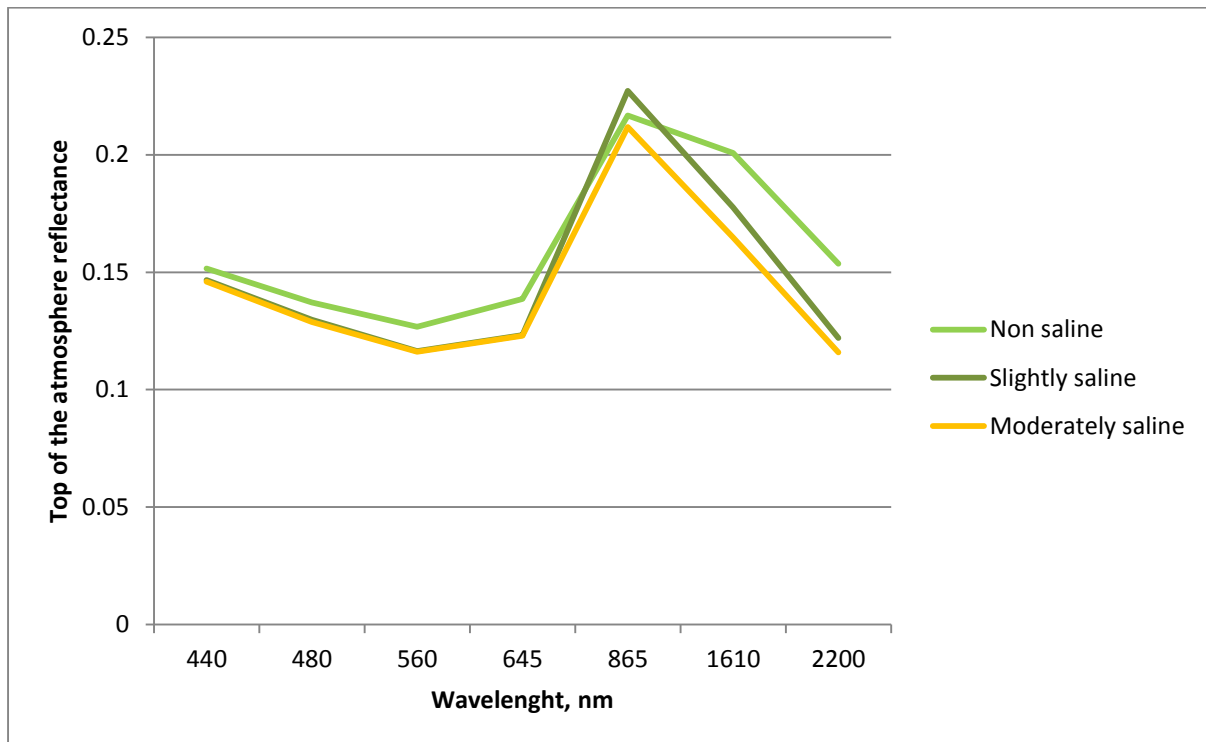
Figure 24. Averaged spectral signatures of soils in Syrdarya region with different salinity levels (Second sampling)

From the spectral signatures analysis we can differentiate non-saline class in all bands, and slightly and moderately saline classes in NIR and SWIR bands (Figure 24). But these patterns not coincide with literature sources, which say that higher salt content lead to higher reflectance level in visible bands. Here we see that highest reflectance can be observed for non-saline class, and slightly saline class shows higher reflectance than moderately saline. This shows that this difference in signature mostly due to difference in soil condition (moisture, roughness, etc.) than salt content.

Table 8. Correlation coefficients of bare soil indices (Second sampling)

Index	Tripathi 1997	IDNP 2002 1	IDNP 2002 2	IDNP 2002 3	Douaoui 2006 1	Douaoui 2006 2	Bouaziz 2011	Abbas 2013 1	Abbas 2013 2	Abbas 2013 3	Abbas 2013 4
R	-0.26	0.30	0.43	0.30	-0.36	-0.36	-0.20	0.34	0.34	-0.35	-0.37

Correlation analysis shows that R values higher in data of second sampling (Table 8), but they still not very high, highest R value is 0.43. In general these R values close to the values that we see in correlation analysis of the archive map (section 3.4).

As the main result of the second sampling we can say that even with improved methods bare soil indices still showing low performance in Syrdarya province.

All obtained results showed us that use of the multispectral satellite images of bare soil cannot give satisfactory results in soil salinity assessment. We test several indices that were found in literature and also implement correlation analysis of individual bands for Landsat 8 images. All R values were below 0.45, which is not enough for reliable and valid estimation. It is possible that use of hyperspectral imagery can improve results of bare soil analysis. Hyperspectral images were used for mineral detection, different material detection and it is very likely that specific absorption features of salts minerals can be detected and recognised on spectral signatures of a hyperspectral data.

But hyperspectral data still not widely available and we should try to use multispectral data as much as possible. For this reason we propose to continue research of vegetation reflectance in relation to soil salinity. Our results showed higher correlation of vegetation indices with EC values in all datasets, highest R^2 value was -0.57 for COSRI index.

4. Conclusions and recommendations

This research shows that remote sensing derived bare soil indices do not show a significant correlation with the soil salinity when applied on soils of Syrdarya province of Uzbekistan. The highest correlation is found when the index from Abbas et al. (2013) are related to the soil salinity level derived from the archive soil map and when index from Indo-Dutch Network Project (2002) related to the soil salinity data gathered during our field campaign. The same results we can see in spectral signatures analysis part, where no differences were discovered between spectral signatures of slightly, moderately and highly saline soils.

Results with vegetation reflectance analysis showed higher correlation. Best R value was achieved with COSRI index (-0.57) in dataset of secondary data. NDVI also showed significant correlation -0.53.

Also important that in all calculations dataset derived from archive map (secondary data) performed almost as good as our data, R values was close in two datasets. So we can conclude that data, which research organisation producing now and different governmental body using, can be imported into GIS environment, for analysis, improving or validation of RS data. This is positive outcome, since we would like to propose our methods to these organisations for improvement of their workflow.

Moreover, according to this better performance of archive map dataset analysis in some cases, we can assume that on a broader scale (farm scale at least) this methods will show better result. This can be explained by more diverse data. When we use dataset for the whole farm we take into account effects of different management practices on different fields, use of different fertilizers, small changes in soil type and soil texture, which still exists, relief change. All

this factors can influence an outcome of the research and cannot be taken into account when we work with individual fields only.

In general we could say that more promising technique for soil salinity assessment by multispectral (like Landsat) RS is vegetation reflectance study. And this could be the direction for future research on soil salinity assessment by RS in Uzbekistan.

References

Abbas, A., Khan, S., Hussain, N., Hanjra, M.A., & Akbar, S. (2013). Characterizing soil salinity in irrigated agriculture using a remote sensing approach. *Physics and Chemistry of the Earth, Parts A/B/C, 55-57*, 43-52

Akramova, I. (2008). Mapping spatial distribution of soil salinity using Remote Sensing and GIS. In, *Laboratory of Geo-Information Science and Remote Sensing* (p. 62). Wageningen, The Netherlands: Wageningen University and Research Centre

Al-Hassoun, S.A. (2010). Remote Sensing Of Soil Salinity In An Arid Areas. *International Journal of Civil & Environmental Engineering, 10 (2)*, 11-20

Al-Khaier, F. (2003). Soil Salinity Detection Using Satellite Remote Sensing. In (p. 61). Enschede, The Netherlands: International Institute For Geo-Information Science And Earth Observation

Al-Mulla, Y.A. (2010). Salinity Mapping in Oman using Remote Sensing Tools: Status and Trends. *A Monograph on Management of Salt-Affected Soils and Water for Sustainable Agriculture* (pp. 17-24): Sultan Qaboos University

Alavi Panah, S.K., Goossens, R., Matinfar, H.R., Mohamadi, H., Ghadiri, M., Irannegad, H., & Alikhah Asl, M. (2008). The Efficiency of Landsat TM and ETM+ Thermal Data for Extracting Soil Information in Arid Regions. *Journal of Agricultural Science and Technology, 10*, 439-460

Aldakheel, Y.Y., Elprince, A.M., & Aatti, M.A. (2006). Mapping vegetation and saline soil using ndvi in arid irrigated lands. In, *ASPRS 2006 Annual Conference*. Reno, Nevada

Bannari, A., Guedon, A.M., El-harti, A., Cherkaoui, F.Z., El-ghmari, A., & Saquaque, A. (2007). Slight And Moderate Saline And Sodic Soils Characterization In Irrigated Agricultural Land Using Multispectral Remote Sensing. *The International Archives of the Photogrammetry, Remote Sensing and Spatial Information Sciences, 34*

Ben-Dor, E., Chabrillat, S., Demattê, J.A.M., Taylor, G.R., Hill, J., Whiting, M.L., & Sommer, S. (2009). Using Imaging Spectroscopy to study soil properties. *Remote Sensing of Environment, 113*, S38-S55

Bouaziz, M., Matschullat, J., & Gloaguen, R. (2011). Improved remote sensing detection of soil salinity from a semi-arid climate in Northeast Brazil. *Comptes Rendus Geoscience, 343*, 795-803

Bucknall, J., Klytchnikova, I., Lampietti, J., Lundell, M., Scatasta, M., & Thurman, M. (2003). Irrigation in Central Asia. Social, Economic and Environmental Considerations. In (p. 104): World Bank

Dehni, A., & Lounis, M. (2012). Remote Sensing Techniques for Salt Affected Soil Mapping: Application to the Oran Region of Algeria. *Procedia Engineering, 33*, 188-198

Ding, J.-l., Wu, M.-c., & Tiyip, T. (2011). Study on Soil Salinization Information in Arid Region Using Remote Sensing Technique. *Agricultural Sciences in China, 10*, 404-411

Douaoui, A.E.K., Nicolas, H., & Walter, C. (2006). Detecting salinity hazards within a semiarid context by means of combining soil and remote-sensing data. *Geoderma, 134*, 217-230

Dutkiewicz, A., Lewis, M., & Ostendorf, B. (2009). Evaluation and comparison of hyperspectral imagery for mapping surface symptoms of dryland salinity. *International Journal of Remote Sensing, 30*, 693-719

Eddine, M.D., Abdelkader, D., & Ibrahim, Y. (2012). Geomatics Use in the Evaluation of Surface Qualities Degradation in Saline Area (The case of the lower Cheliff plain). *Energy Procedia, 18*, 1557-1572

Eldiery, A., Garcia, L.A., & Reich, R.M. (2005). Estimating Soil Salinity from Remote Sensing Data in Corn Fields. *Hydrology Days, 2005*, 31-42

Elhaddad, A., & Garcia, L.A. (2009). *Remote sensing application in agriculture. Using remote sensing to estimate soil salinity and evapotranspiration*. VDM Publishing House Ltd.

Fernández-Buces, N., Siebe, C., Cram, S., & Palacio, J.L. (2006). Mapping soil salinity using a combined spectral response index for bare soil and vegetation: A case study in the former lake Texcoco, Mexico. *Journal of Arid Environments, 65*, 644-667

Ghassemi, F., Jakeman, A., & Nix, H. (1995). *Salinization of land and water resources: human causes, extent, management and case studies, Canberra, Australia*. Wallingford, Oxon, UK: CAB International

Goskomgeodezkadastr (2010). Atlas of soil cover of Republic of Uzbekistan. In. Tashkent, Uzbekistan

Gutierrez, M., & Johnson, E. (2010). Temporal variations of natural soil salinity in an arid environment using satellite images. *Journal of South American Earth Sciences, 30*, 46-57

Hamzeh, S., Naseri, A.A., AlaviPanah, S.K., Mojaradi, B., Bartholomeus, H.M., Clevers, J.G.P.W., & Behzad, M. (2013). Estimating salinity stress in sugarcane fields with spaceborne hyperspectral vegetation indices. *International Journal of Applied Earth Observation and Geoinformation, 21*, 282-290

Howari, F.M. (2003). The use of remote sensing data to extract information from agricultural land with emphasis on soil salinity. *Australian Journal of Soil Research, 41*, 1243-1253

Indo-Dutch Network Project, I. (2002). *A Methodology for Identification of Waterlogging and Soil Salinity Conditions Using Remote Sensing*. Karnal, India and Wageningen, The Netherlands

Iqbal, S., Iqbal, F., & Iqbal, F. (2010). Satellite Sensing for Evaluation of an Irrigation System in Cotton - Wheat Zone. *World Academy of Science, Engineering and Technology, 71*, 261-266

Ivushkin, K.A. (2012). Soil salinity assessment using Remote Sensing techniques. In (p. 19). Tashkent, Uzbekistan: Tashkent Institute of Irrigation and Melioration

Karavanova, E.I., Shrestha, D.P., & Orlov, D.S. (2001). Application of remote sensing techniques for the study of soil salinity in semi-arid Uzbekistan. In e.a. Bridges (Ed.), *Response to Land Degradation* (pp. 261-273): Oxford & IBH Publishing Co. Pvt. Ltd.

Karimov, I. (2014). Cabinet of Ministers meeting on social and economical development of Uzbekistan in 2013. In. Tashkent, Uzbekistan

Koshal, A.K. (2012). Spectral characteristics of soil salinity areas in parts of South – West Punjab through Remote Sensing and GIS. *International Journal of Remote Sensing and GIS, 1*, 84-89

Mashimbye, Z.E., Cho, M.A., Nell, J.P., De Clercq, W.P., Van Niekerk, A., & Turner, D.P. (2012). Model-Based Integrated Methods for Quantitative Estimation of Soil Salinity from Hyperspectral Remote Sensing Data: A Case Study of Selected South African Soils. *Pedosphere, 22*, 640-649

Mehrjardi, R.T., Mahmoodi, S., Taze, M., & Sahebjalal, E. (2008). Accuracy Assessment of Soil Salinity Map in Yazd-Ardakan Plain, Central Iran, Based on Landsat ETM+ Imagery. *American-Eurasian Journal of Agricultural & Environmental Sciences, 3 (5)*, 708-712

Noroozi, A.A., Homaee, M., & Farshad, A. (2012). Integrated Application of Remote Sensing and Spatial Statistical Models to the Identification of Soil Salinity: A Case Study from Garmsar Plain, Iran. *Environmental Sciences, 9 (1)*, 59-74

Ochieng, G.M., Ojo, I.O., Otieno, F.A.O., & Mwaka, B. (2013). Use of remote sensing and geographical information system (GIS) for salinity assessment of Vaal-Harts irrigation scheme, South Africa. *Environmental Systems Research, 2 (4)*

Pattanaaik, S.K., Singh, O.P., Sahoo, R.N., & Singh, D.K. (2008). Irrigation Induced Soil Salinity Mapping through Principal Component Analysis of Remote Sensing Data. *Journal of Agricultural Physics, 8*, 29-36

Robbins, C.W., & Wiegand, C.L. (1990). Field and laboratory measurements, Agricultural Salinity Assessment and Management. *American Society of Civil Engineers*

Sanaeinejad, S.H., Astaraei, A., Mirhoseini, P., Mousavi, & Ghaemi, M. (2009). Selection of Best Band Combination for Soil Salinity Studies using ETM+ Satellite Images (A Case study: Nyshaboor Region,Iran). *World Academy of Science, Engineering and Technology, 54*, 519-521

Shrestha, R.P. (2006). Relating soil electrical conductivity to remote sensing and other soil properties for assessing soil salinity in northeast Thailand. *Land Degradation & Development, 17*, 677-689

Singh, P., & Somvanshi, S. (2012). Integrated Remote Sensing And Gis Approach For Determining Soil Salinity. In, *13th Esri India User Conference 2012*

State Research Institute of Soil Science and Agrochemistry, S. (2005). *Arable soils of Syrdarya and Jizzakh*. FAN

The World Bank (2007). Integrating Environment into Agriculture and Forestry. Progress and Prospects in Eastern Europe and Central Asia. UZBEKISTAN. In (p. 12)

Toderich, K., Tsukatani, T., Shoaib, I., Massino, I., Wilhelm, M., Yusupov, S., Kuliev, T., & Ruziev, S. (2008). Extent of Salt Affected Land in Central Asia: Biosaline Agriculture and Utilization of the Salt-affected Resources. *KIER DISCUSSION PAPER SERIES*, 34

Tripathi, N.K., Rai, B.K., & Dwivedi, P. (1997). Proceedings. In, *18th Asian Conference in Remote Sensing* (pp. A-8-1–A-8-6). Kuala Lumpur, Malaysia

UNDP (2009). National Irrigated Land Reclamation Fund Capacity Development, Project document. In

USGS (2013). Landsat 8. In (p. 4)

Volkmar, K.M., Hu, Y., & Steppuhn, H. (1998). Physiological responses of plants to salinity: A review. *Canadian Journal of Plant Science, 78*, 19-27

Wang, F., Chen, X., Luo, G., Ding, J., & Chen, X. (2013). Detecting soil salinity with arid fraction integrated index and salinity index in feature space using Landsat TM imagery. *Journal of Arid Land, 5*, 340-353

Watling, K. (2007). Measuring salinity. Fact sheet. In N.R.a. Water (Ed.): Queensland Government

Weng, Y.-L., Gong, P., & Zhu, Z.-L. (2010). A spectral Index for Estimating Soil Salinity in the Yellow River Delta Region of China Using EO-1 Hyperion Data. *Pedosphere, 20 (3)*, 378-388

Wu, J., Vincent, B., Yang, J., Bouarfa, S., & Vidal, A. (2008). Remote Sensing Monitoring of Changes in Soil Salinity: A Case Study in Inner Mongolia, China. *Sensors, 8*, 7035-7049

Zehtabian, G.R., Alavipanah, S.K., & Ehsani, A.H. (2002). The Use of Landsat Thematic Mapper Data for Mapping the Marginal Playa Soils in Damghan Playa, IRAN. In, *FIG XXII International Congress*. Washington, D.C. USA

Zhang, T.-T., Zeng, S.-L., Gao, Y., Ouyang, Z.-T., Li, B., Fang, C.-M., & Zhao, B. (2011). Using hyperspectral vegetation indices as a proxy to monitor soil salinity. *Ecological Indicators, 11*, 1552-1562

Zribi, M., Baghdadi, N., & Nolin, M. (2011). Remote Sensing of Soil. *Applied and Environmental Soil Science, 2011*, 1-2